Phase transitions in QCD in the frame of the Field Correlator approach

Yu.A.Simonov et al.

Institute of Theoretical and Experimental Physics, Moscow, Russia

Talk by Dr. Michael Trusov at the CBM meeting, Dubna, Russia, May 2009

Contents

1. Introduction: perturbative vs nonperturbative.
2. Physics of phase transition.
3. Polyakov lines and EoS.
4. $qq, q\bar{q}, gg, 3q$ interaction.
5. Suppression of SC and baryon matter – quark matter transition.
6. Conclusion.

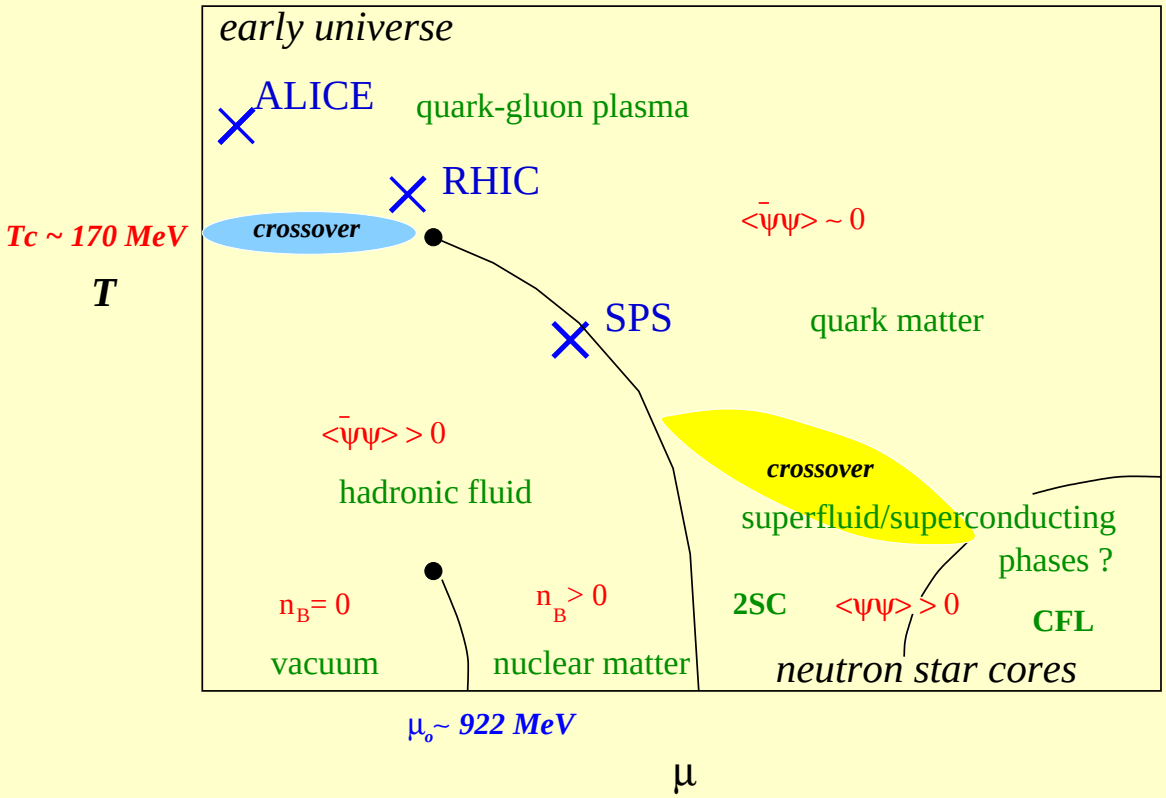

Figure 1: The QCD phase diagram in the temperature-chemical potential plane. First order phase transitions are shown as solid lines, and second order transitions by filled circles. Crosses depict heavy-ion collision experiments. The region of interest in this work is the *crossover* transition at $T_c \approx 170$ MeV.

QCD at $T > T_c$: Perturbative vs Nonperturbative Methods:

1. Perturbative theory using QCD Lagrangian (small T) or effective Lagrangian (beyond dimensional reduction).
2. Models (nonconfining): NJL and modifications.
3. Systematic nonpert. method: Field correlator Method.
4. Lattice calculations (not very reliable for $\mu > 0$).

We shall use 3 and 4 in what follows.

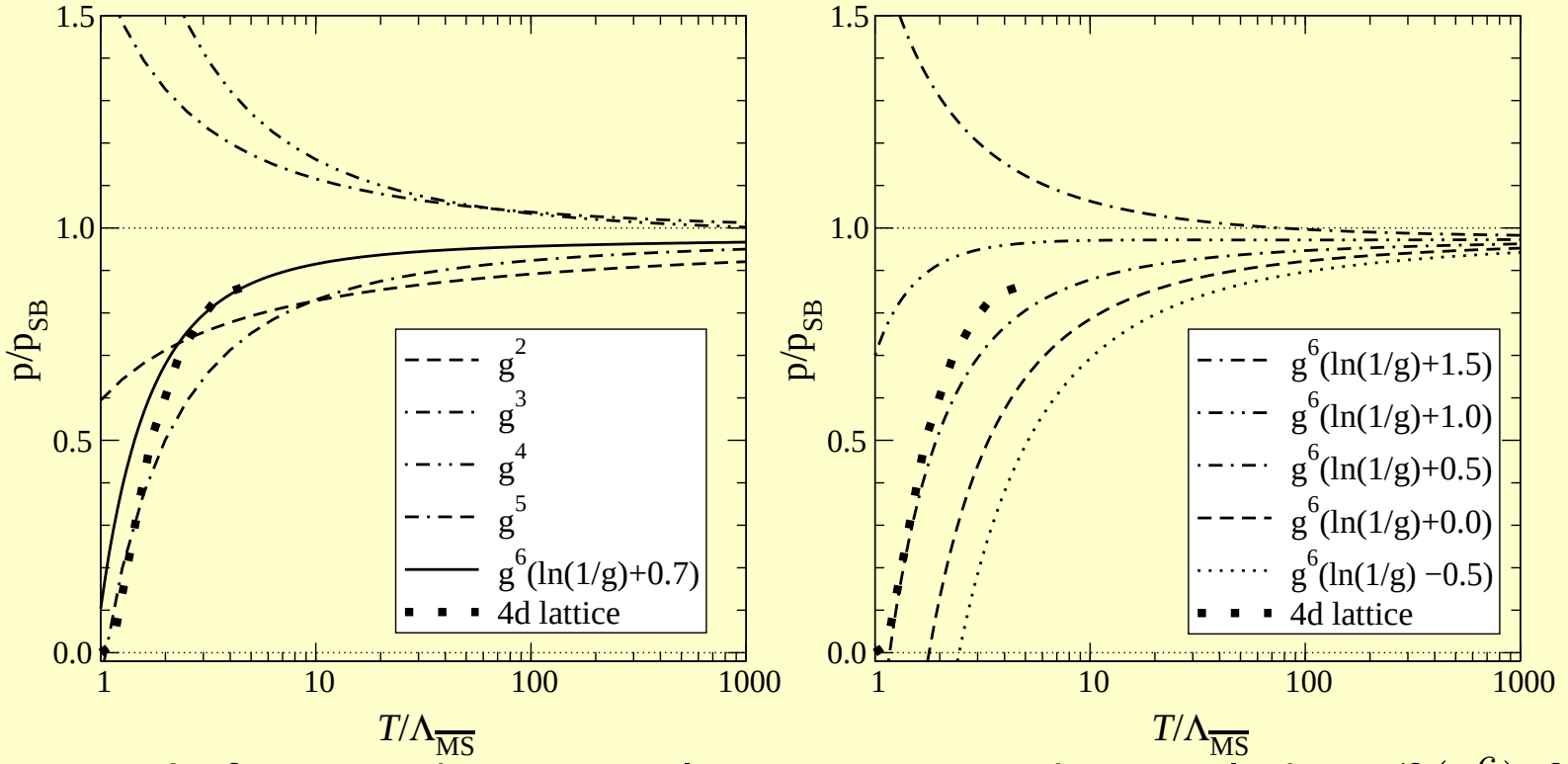

Figure 2: Left: perturbative results at various orders, including $\mathcal{O}(g^6)$ for an optimal constant, normalised to the non-interacting Stefan-Boltzmann value p_{SB}. Right: the dependence of the $\mathcal{O}(g^6)$ result on the (not yet computed) constant, which contains both perturbative and non-perturbative contributions.

Physical picture in terms of correlators

$$g^2\langle\hat{t}r_f[E_i(x)\Phi(x,y)E_k(y)\Phi(y,x)]\rangle$$
$$= \delta_{ik}\left[D^E + D_1^E + u_4^2\frac{\partial D_1^E}{\partial u_4^2}\right] + u_i u_k \frac{\partial D_1^E}{\partial \mathbf{u}^2} \ ,$$

$$g^2\langle\hat{t}r_f[H_i(x)\Phi(x,y)H_k(y)\Phi(y,x)]\rangle$$
$$= \delta_{ik}\left[D^H + D_1^H + \mathbf{u}^2\frac{\partial D_1^H}{\partial \mathbf{u}^2}\right] - u_i u_k \frac{\partial D_1^H}{\partial \mathbf{u}^2} \ ,$$

$$g^2\langle\hat{t}r_f[E_i(x)\Phi(x,y)H_k(y)\Phi(y,x)]\rangle = -\frac{1}{2}\varepsilon_{ikn}u_n\frac{\partial D_1^{HE}}{\partial u_4} \ .$$

Field correlators at $T = 0$ and $T \geq T_c$

All dynamics: Green's functions, energy density etc. can be expressed via field correlators at all T. The lowest one, Gaussian contributes more than 90%

Confinement due to D^E

$$\sigma = \frac{1}{2} \int D^E(x) D^2 x :$$

FC are calculated analytically as gluelump Green's functions (Yu.S.'05) and on the lattice (Pisa group, Wuppertal group,...)

I. Confining phase: correlators D^E, D^H, D_1^E, D_1^H are all nonzero.

At $T = 0$ $D^E = D^H$, $D_1^E = D_1^H$, $\sigma^E = \sigma^H \equiv \sigma_s$

$$\sigma^{(i)} = \frac{1}{2} \int D^{(i)}(x) d^2 x, i = E, H$$

$$D^{(i)}(x) = D^{(i)}(0) \exp\left(-|x|/\lambda\right), \quad \lambda \cong 0.2 \ \text{fm}.$$

Gluonic condensate $G_2 \equiv \frac{\alpha_s}{\pi}\langle (F^a_{\mu\nu})^2 \rangle = G_2^E + G_2^H$

at $T = 0 \;\; G_2^E = G_2^H$ till $T = T_c$.

$G_2 = 0.012$ GeV^4 (SVZ).

S. Narison $G_2 = \frac{1}{\pi}(0.07 \div 0.009)$ GeV^4.

Vacuum energy density

$$\varepsilon = \frac{\beta(\alpha_s)}{16\alpha_s}\langle (F^a_{\mu\nu})^2 \rangle \cong -\frac{11 - \frac{2}{3}n_f}{32} G_2 = \varepsilon^E + \varepsilon^H \quad \varepsilon^E = \varepsilon^H, \quad T = 0$$

II Deconfined phase, $T \geq T_c(\mu)$.

Here only D^E vanishes:

New QCD vacuum state with strong colormagnetic forces.

Colorelectric only in $D_1^E \rightarrow$ Polyakov loops.

Definitions ($H_k \equiv \frac{1}{4}\varepsilon_{ijk}F_{ij}$)

How FC behave below and above T_c?

It is advantageous (minimal $F(T)$) to have vacuum without confining colorelectric fields. Calculation of T_c Simonov, (1991)

$D^E = 0$, $T > T_c$ all others nonzero.

CE gluon condensate vanishes:

Check: Pisa group

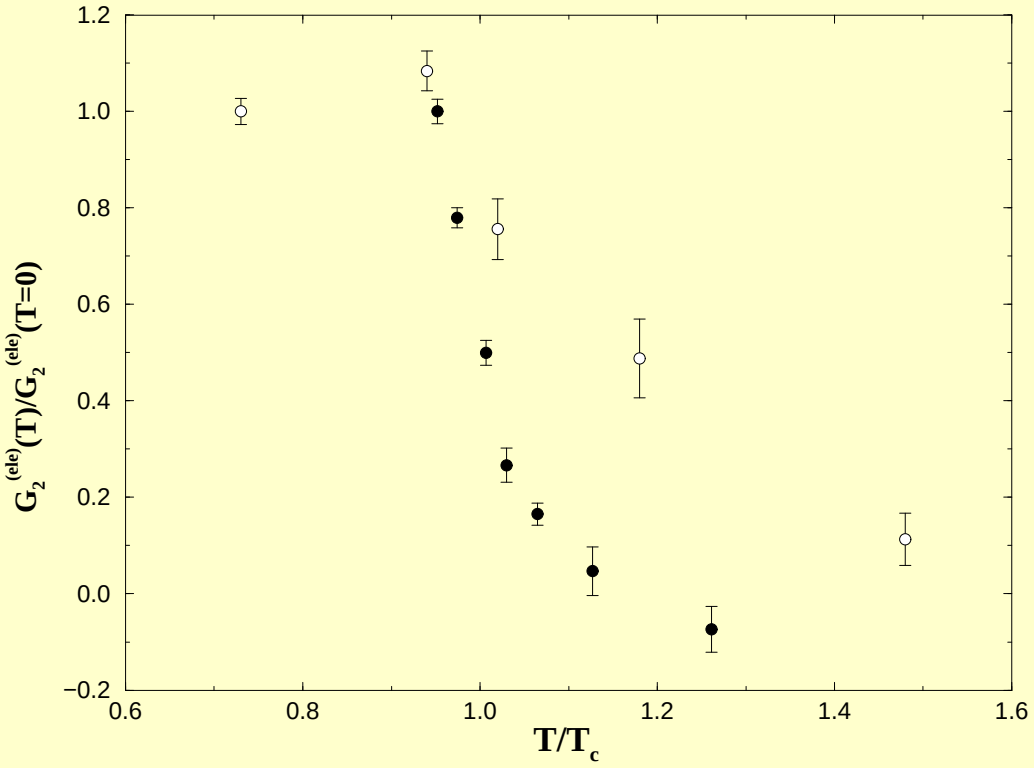

Figure 3: The electric gluon condensate $G_2^{(ele)}(T)$ in units of $G_2^{(ele)}(T = 0)$, versus T/T_c. The black circles refer to the *quenched* case, while the white circles refer to the full–QCD case.

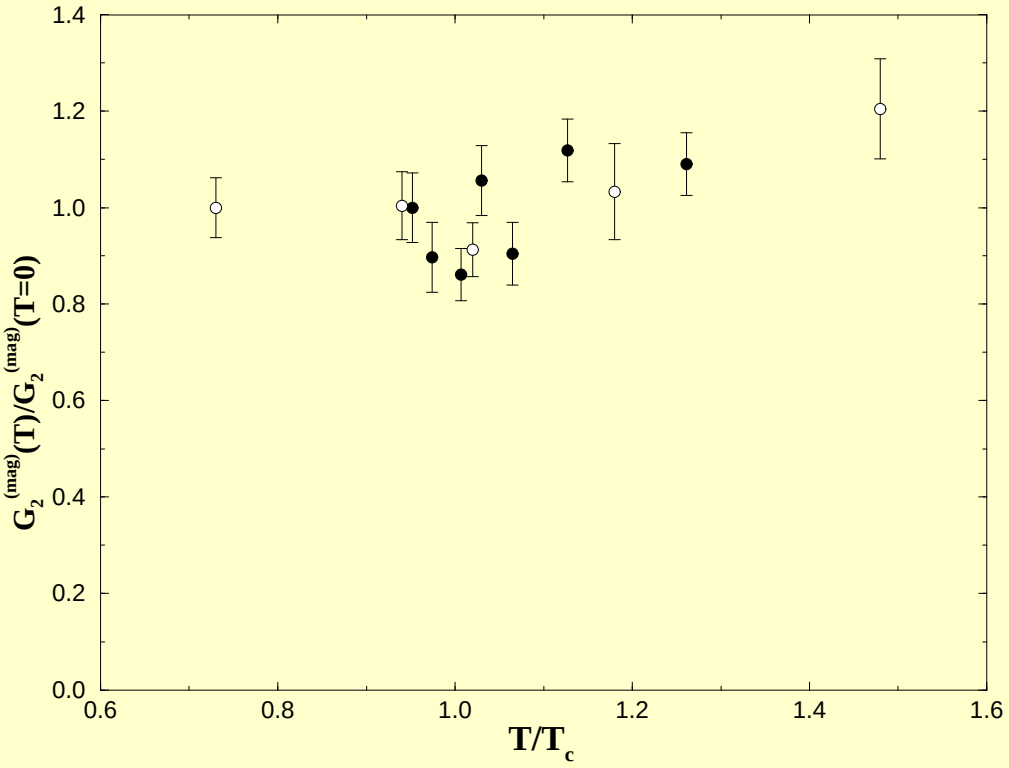

Figure 4: The magnetic gluon condensate $G_2^{(mag)}(T)$ in units of $G_2^{(mag)}(T=0)$, versus T/T_c. The notation is the same as in Fig. 3.

Gauge invariance at $T > 0$. Consequence:

No $Z(N_c)$ symmetry violation.

Only $|L_{fund}|$ finally enter because of gauge invariance.

Here L_i - Polyakov lines

$$L_{fund} = trP \exp(ig \int_0^{1/T} A_4 dz_4), L_{adj}$$

L_{fund} for quark, L_{adj} for gluons play important dynamical role: they create nonperturbative self-energy of quarks and gluons which defines EoS in first approximation.

Vacuum Dominance Scheme of approximation

First step: Vacuum energy density and interaction of individual gluons and quarks with vacuum is taken into account.

Second step: Pair and triple interaction meditated by vacuum is taken into account.

Perturbative to $O(\alpha_s)$.

Higher orders.

Result: EoS in terms of one-particle propagators, modified by vacuum $\longrightarrow$ modulus of Polyakov loop.

Qualitative check:

Correlations of quark quantum numbers – QNS.

Single Line Approximation

Using $P_{gl}V_3 = -\langle F_0(B)\rangle_B$

$$P_{gl} = (N_c^2 - 1)\int_0^\infty \frac{ds}{s}\sum_{n\neq 0} G^{(n)}(s) \tag{1}$$

$$P_q = 2N_c\int_0^\infty \frac{ds}{s}e^{-m_q^2 s}\sum_{n=1}^{\infty}(-1)^{n+1}[S^{(n)}(s) + S^{(-n)}(s)]. \tag{2}$$

$$G^{(n)}(s) = \int (Dz)^w_{on} e^{-K}\hat{tr}_a\langle W_\Sigma(C_n)\rangle \tag{3}$$

$$S^{(n)}(s) = \int \overline{(Dz)}^w_{on} e^{-K}\hat{tr}_f\langle W_\sigma(C_n)\rangle \tag{4}$$

$$\hat{tr}_f W_\sigma(C_n) = \frac{1}{N_c} tr_f W_\sigma(C_n) \tag{5}$$

and

$$\hat{tr}_a \langle W_\Sigma(C_n)\rangle = \frac{tr_a}{(N_c^2-1)}(\frac{1}{2}\tilde{\Phi}_F(C_n) - \tilde{\Phi}(C_n)) \qquad (6)$$

Expansion in Field Correlators –take Gaussian approximation.

$$\hat{tr}_f \langle W(C_n)\rangle = \frac{tr_c}{N_c}\langle P \exp ig \int_{C_n} B_\mu dz_\mu\rangle =$$

$$= \frac{tr_c}{N_c}\exp\left(-\frac{g^2}{2}\int_{S_n}\int_{S_n} d\sigma_{\mu\nu}(u) d\sigma_{\lambda\sigma}(v)\langle F_{\mu\nu}(u)F_{\lambda\sigma}(v)\rangle\right). \qquad (7)$$

Resulting pressure in SLA is (we neglect colormagnetic contribution and write $G_3^{(0)}(s) = \frac{1}{(4\pi s)^{3/2}} = S_3^{(0)}(s)$

$$P_{gl}^{(0)} = \frac{(N_c^2-1)}{2\sqrt{\pi}}\int_0^\infty \frac{ds}{s^{3/2}} G_3(s) \sum_{n\neq 0} e^{-\frac{n^2}{4T^2 s}} L_{adj}^{(n)} =$$

$$= \frac{(N_c^2-1)}{16\pi^2}\int_0^\infty \frac{ds}{s^3}\sum_{n\neq 0} e^{-\frac{n^2}{4T^2 s}} e^{-\tilde{J}_n^E} \qquad (8)$$

$$P_q^{(0)} = \frac{2N_c}{\sqrt{\pi}} n_f \int_0^\infty \frac{ds}{s^{3/2}} e^{-m_q^2 s} S_3(s) \sum_{n=1}^\infty (-1)^{n+1} e^{-\frac{n^2}{4T^2 s}} L_{fund}^{(n)} cosh\frac{\mu n}{T} =$$

$$= n_f \frac{N_c}{4\pi^2} \int_0^\infty \frac{ds}{s^3} e^{-m_q^2 s} \sum_{n=1}^\infty (-1)^{n+1} e^{-\frac{n^2}{4T^2 s}} e^{-J_n^E} cosh\frac{\mu n}{T}, \qquad (9)$$

Check: free gas: $m_q = 0, \mu = 0, L_i = 1.$

Using

$$\sum_{n=1}^\infty \frac{1}{n^4} = \frac{\pi^4}{90}, \quad \sum_{n=1}^\infty \frac{(-1)^{n+1}}{n^4} = \frac{7\pi^4}{720}. \qquad (10)$$

one has Stefan-Boltzmann result

$$P_{gl}^{SB}(\sigma \to 0) = \frac{\pi^2 (N_c^2 - 1) T^4}{45}, \quad P_q^{SB}(\sigma \to 0) = \frac{7\pi^2 N_c T^4}{180} n_f, \qquad (11)$$

Taking L_i into account and $L_i^{(n)} = (L_i)^n$ for $T < 1$ GeV $= \frac{1}{\lambda_{gl}}$

$$P_{gl}^{(0)} = \frac{(N_c^2-1)T^4}{\pi^2} \sum_{n\neq 0} \frac{(L_{adj})^{|n|}}{n^4} \approx \frac{2(N_c^2-1)}{\pi^2} L_{adj} T^4 \qquad (12)$$

$$P_q^{(0)} = \frac{4N_c n_f}{\pi^2} \sum_{n=1}^{\infty} \frac{(-1)^n}{n^4} \varphi_q^{(n)}(T) cosh \frac{\mu n}{T} \approx$$

$$\approx \frac{4N_c}{\pi^2} n_f L_{fund} T^4 \varphi_q^{(1)}(T) cosh \frac{\mu}{T} \qquad (13)$$

$$\varphi_q^{(n)}(T) = \frac{1}{16T^4} \int_0^{\infty} \frac{ds}{s^3} e^{-m_q^2 s} e^{-\frac{1}{4T^2 s}} \cong$$

$$\cong \frac{n^2 m_q^2}{2T^2} K_2 \left(\frac{m_q n}{T} \right), \qquad (14)$$

$$P_g = T^4 p_g; \quad P_q = T^4 p_q;$$

$$p_g = \frac{16}{\pi^2} L_{adj}(T) = \frac{16}{\pi^2} \exp\left(-\frac{9V_1(\infty, T)}{8T}\right) \tag{15}$$

$$p_q = \frac{12 n_f}{\pi^2} \sum_{n=1}^{\infty} \frac{(-)^{n+1}}{n^4} (L_f)^n \varphi_q^{(n)}(T) ch\frac{\mu n}{T} \tag{16}$$

$$m_q = 0$$

$$p_q(m_q = 0) = \frac{12 n_f}{\pi^2} \sum_{n=1}^{\infty} \frac{(-)^{n+1}}{n^4} L_f^n ch\frac{\mu n}{T} =$$

$$= \frac{n_f}{\pi^2} \left[\Phi_-^{(3)}\left(\frac{\mu - \frac{V_1}{2}}{T}\right) + \Phi_+^{(3)}\left(\frac{\mu + \frac{V_1}{2}}{T}\right)\right] \tag{17}$$

$$T_c = \left[\frac{|\frac{\varepsilon}{2}| + \chi_1(T)}{p_g + p_q}\right]^{1/4}$$

$$\Phi_-^{(k)}(z) = \int_0^\infty \frac{x^k dx}{e^{x-z}+1}; \quad \Phi_+^{(k)}(z) = \int_0^\infty \frac{x^k dx}{e^{x+z}+1}; \qquad (18)$$

$$|L_{fund}| = \exp\left(-\frac{V_1}{2T}\right).$$

Properties of Polyakov loops

$$G^{(n)}(s) = \frac{1}{2\sqrt{\pi s}} e^{-\frac{n^2\beta^2}{4s}} G_3(s) L^{(n)}_{adj} \tag{19}$$

$$L^{(n)}_{adj} \equiv \exp(-\tilde{J}^E_n), \quad \tilde{J}^E_n = \frac{9}{4} J^E_n \tag{20}$$

$$J^E_n = \frac{n\beta}{2} \int_0^{n\beta} d\nu \left(1 - \frac{\nu}{n\beta}\right) \int_0^{\infty} \xi d\xi D^E_1(\sqrt{\nu^2 + \xi^2}). \tag{21}$$

$$L_{fund} = \exp\left(-\frac{1}{2T} V_1(\infty)\right), \quad \frac{1}{2T} V_1(\infty) \equiv J^E_1 \tag{22}$$

$$D^E_1(x) = D^E_{1pert}(x) + D^E_{1nonp.}(x) \tag{23}$$

$$D^E_{1nonp}(x) \approx const \exp(-M_1|x|), |x| \gtrsim 1/M_1 \tag{24}$$

Below and above $\mathbf{T_c}$:

(also D^E is nonzero below T_c)

$$V_D(r,T) = 2\int_0^\beta d\nu(1-\nu T)\int_0^r (r-\xi)d\xi D^E(\sqrt{\xi^2+\nu^2}) \qquad (25)$$

$$L_{fund} = \exp\{-(V_D(r_1^*,T) + \frac{1}{2}V_1^{np}(\infty,T))/T\}, \quad L_{adj} = (L_{fund})^{9/4} \qquad (26)$$

r_1^* – average radius of heavy-light meson (of gluelump for L_{adj})

$r^* \approx 0.5$ fm (0.3 fm) for $fund$ (adj)

$$V_1^{(np)}(\infty,T) = \int_0^\beta d\nu(1-\nu T)\int_0^\infty \xi d\xi D_{1np}(\sqrt{\xi^2+\nu^2});$$

Check 1: Casimir scaling: $(V_D, V_1)_{adj} = \frac{9}{4}(V_D, V_1)_{fund}$;

for higher repr. of $SU(3)_c$; $\frac{9}{4} \to \frac{C_2(j)}{C_2(fund)}$

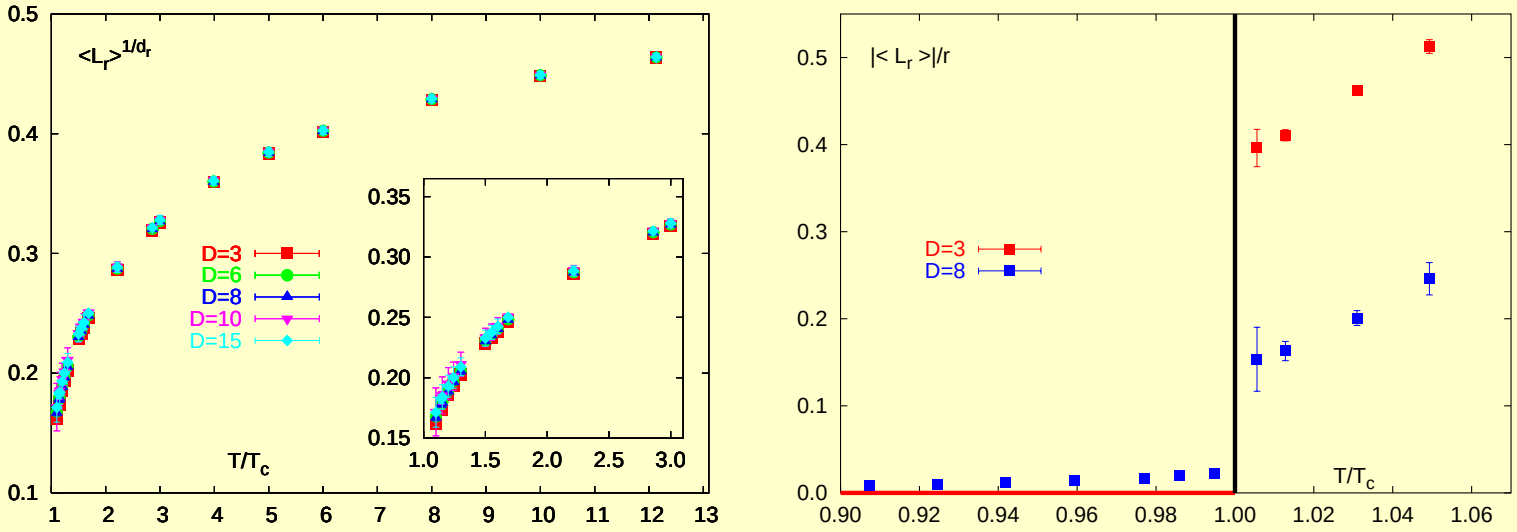

Figure 5: Left: bare Polyakov loops for $r \leq 15$ with cubic spline above T_c. Right: renormalized fundamental and adjoint Polyakov loop for temperatures around T_c.

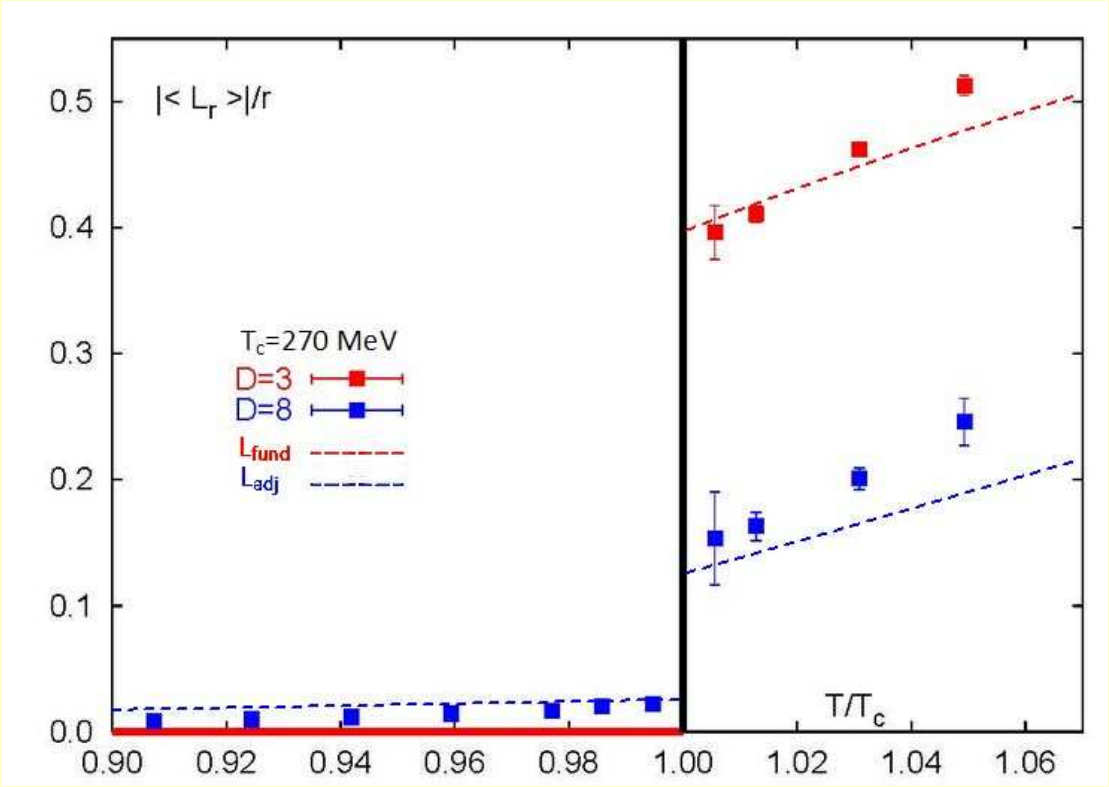
|< L_r >|/r
T_c=270 MeV
D=3
D=8
L_fund
L_adj
T/T_c
0.0
0.1
0.2
0.3
0.4
0.5
0.90
0.92
0.94
0.96
0.98
1.00
1.02
1.04
1.06

Figure 6:

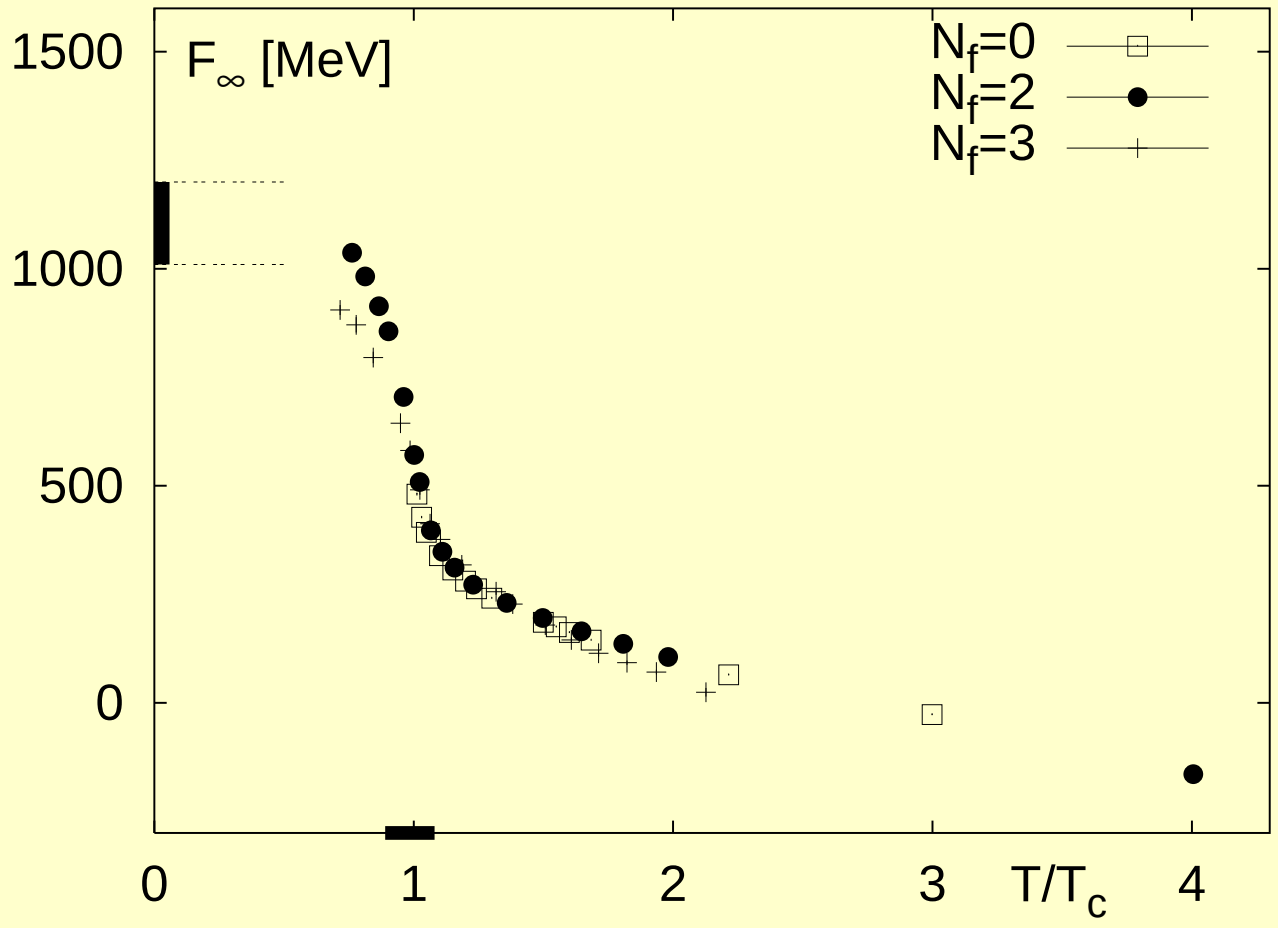

Figure 7:

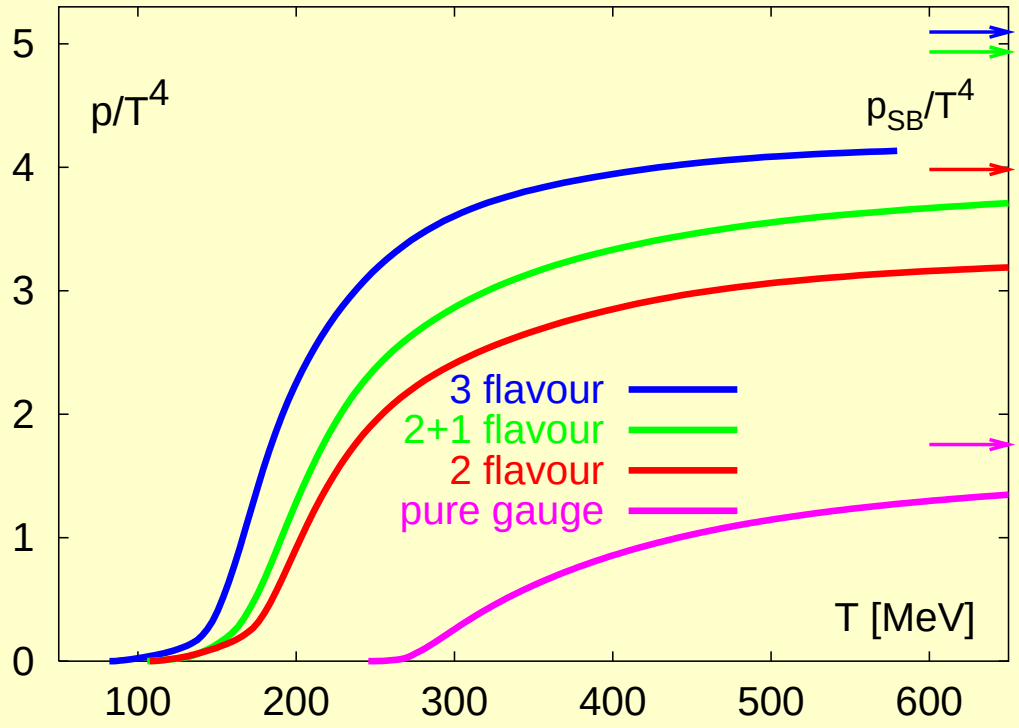
p/T^4
p_SB/T^4
3 flavour
2+1 flavour
2 flavour
pure gauge
T [MeV]
0
1
2
3
4
5
100
200
300
400
500
600

Figure 8:

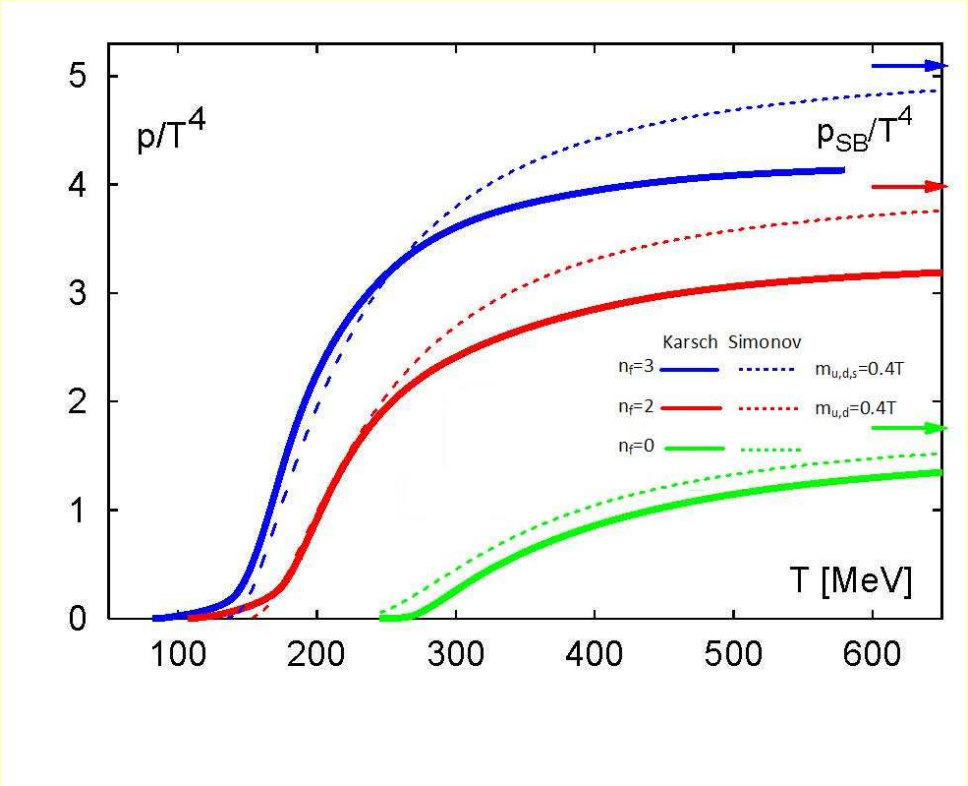
p/T^4
p_SB/T^4
Karsch Simonov
n_f=3
m_u,d,s=0.4T
n_f=2
m_u,d=0.4T
n_f=0
T [MeV]
0
1
2
3
4
5
100
200
300
400
500
600

Figure 9:

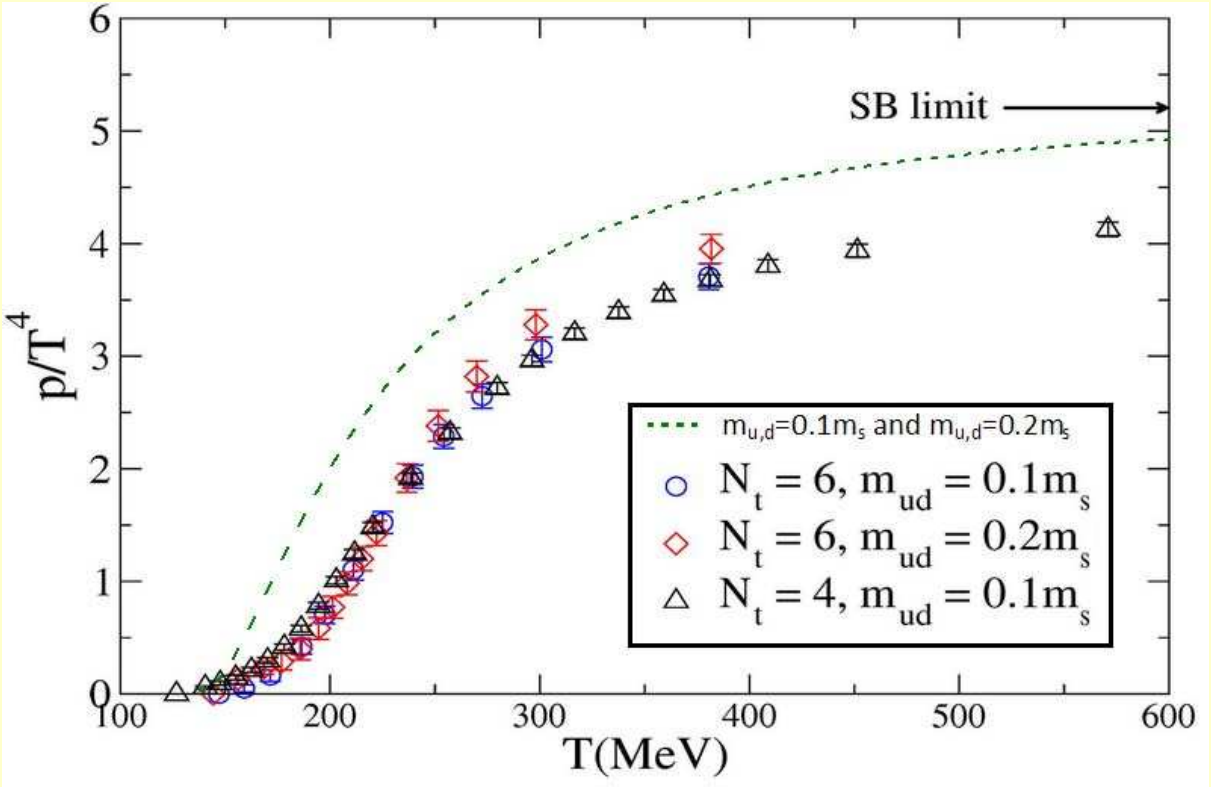
SB limit
$m_{u,d}=0.1m_s$ and $m_{u,d}=0.2m_s$
$N_t = 6, m_{ud} = 0.1m_s$
$N_t = 6, m_{ud} = 0.2m_s$
$N_t = 4, m_{ud} = 0.1m_s$
p/T^4
T(MeV)
0
1
2
3
4
5
6
100
200
300
400
500
600

Figure 10:

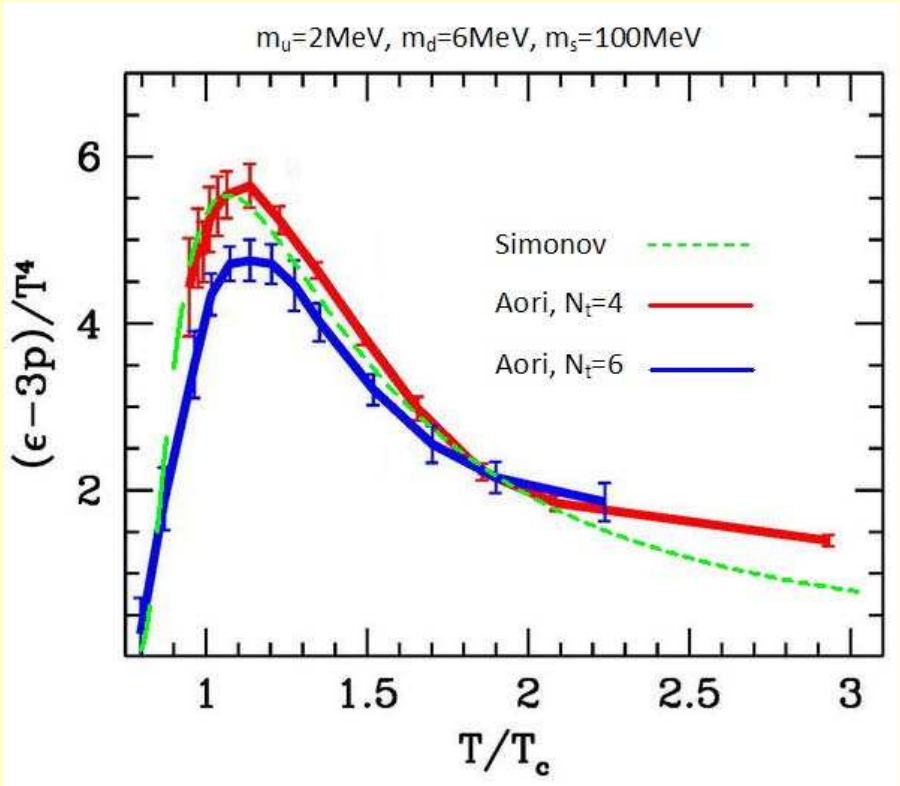
m_u=2MeV, m_d=6MeV, m_s=100MeV
Simonov
Aori, N_t=4
Aori, N_t=6
$(\epsilon-3p)/T^4$
T/T_c
6
4
2
1
1.5
2
2.5
3

Figure 11:

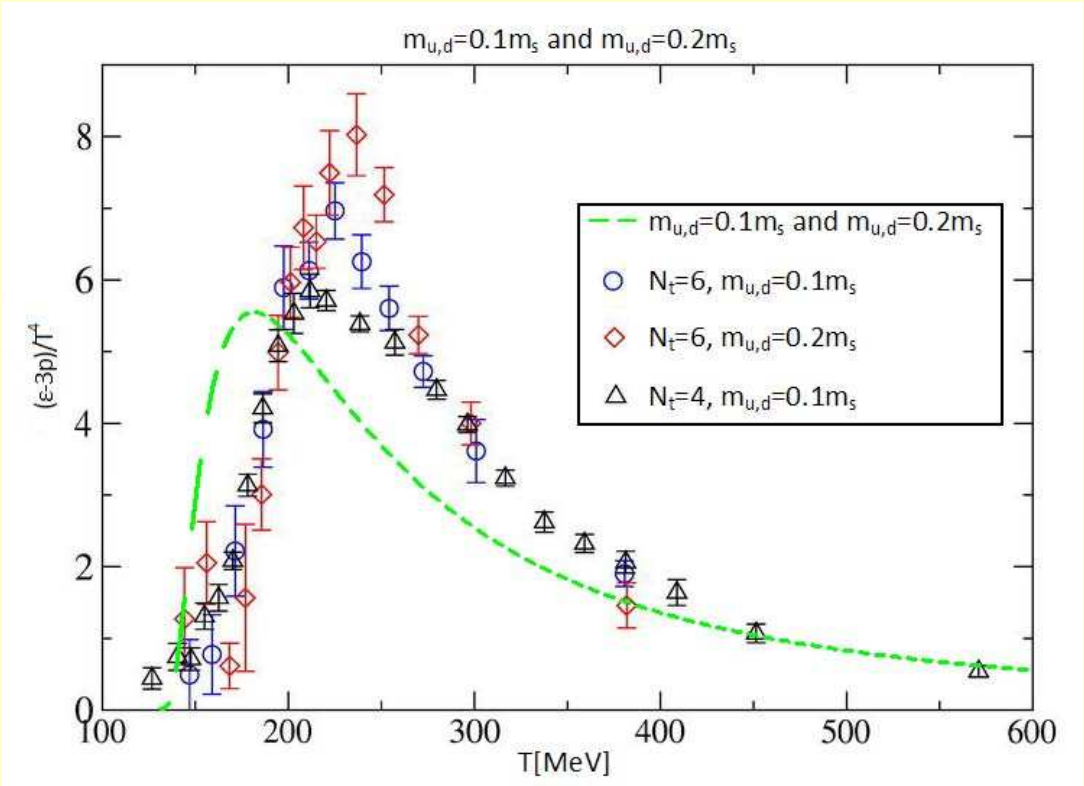
$m_{u,d}=0.1m_s$ and $m_{u,d}=0.2m_s$
$(\varepsilon-3p)/T^4$
T[MeV]
$m_{u,d}=0.1m_s$ and $m_{u,d}=0.2m_s$
$N_t=6$, $m_{u,d}=0.1m_s$
$N_t=6$, $m_{u,d}=0.2m_s$
$N_t=4$, $m_{u,d}=0.1m_s$

Figure 12:

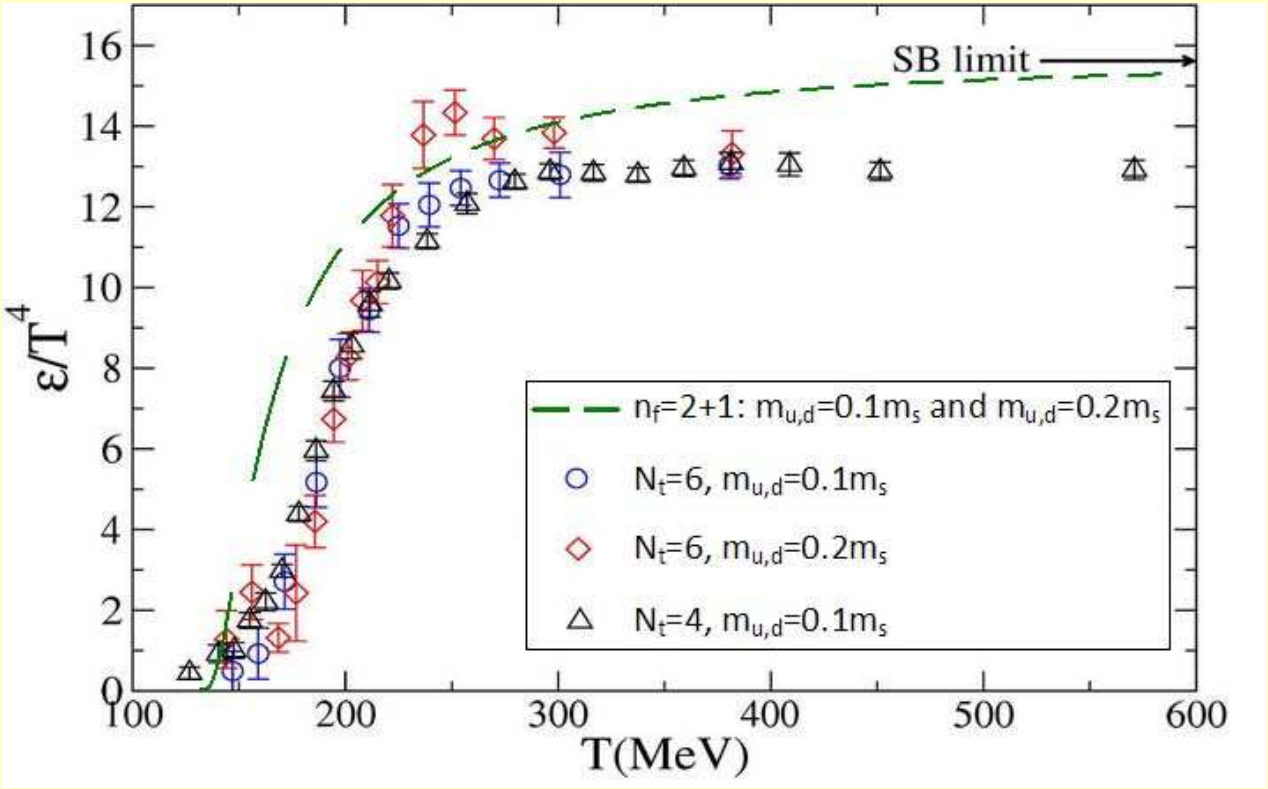
SB limit
n_f=2+1: $m_{u,d}$=0.1m_s and $m_{u,d}$=0.2m_s
N_t=6, $m_{u,d}$=0.1m_s
N_t=6, $m_{u,d}$=0.2m_s
N_t=4, $m_{u,d}$=0.1m_s
ε/T^4
T(MeV)
0
2
4
6
8
10
12
14
16
100
200
300
400
500
600

Figure 13:

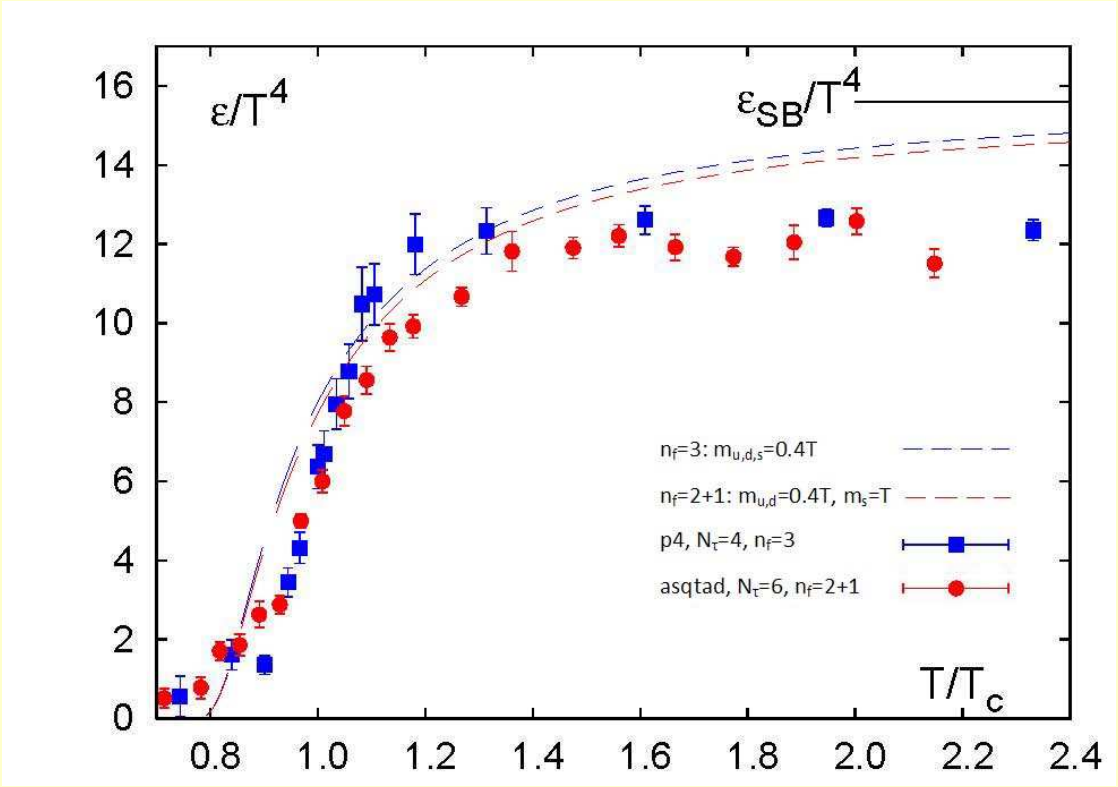
ε/T^4
ε_SB/T^4
n_f=3: m_u,d,s=0.4T
n_f=2+1: m_u,d=0.4T, m_s=T
p4, N_τ=4, n_f=3
asqtad, N_τ=6, n_f=2+1
T/T_c
0
2
4
6
8
10
12
14
16
0.8
1.0
1.2
1.4
1.6
1.8
2.0
2.2
2.4

Figure 14:

Phase transition: Equation for $T_c(\mu)$ M.A.Trusov and Yu.S.

$$SVZ \quad \varepsilon_{vac} = 1/4\theta_{\mu\mu} = \frac{\beta(\alpha_s)}{16\alpha_s}\langle (F^a_{\mu\nu})^2\rangle \cong -\frac{(11-\frac{2}{3}n_f)}{32}G_2^{(n_f)} \tag{27}$$

$$(NSVZ) \quad G_2^{(n_f=2)} \approx \left(\frac{1}{3} \div \frac{1}{4}\right) G_2^{(n_f=0)} \tag{28}$$

$$G_2 = (0.02 \pm 0.005)\ GeV^4 \text{ S.Narison}$$
$$G_2 = (0.01 \pm 0.002)\ GeV^4 \text{ Andreev, Zakharov} \tag{29}$$

$$P_1(T) = |\varepsilon_{vac}| + \frac{\pi^2}{30}T^4 + T\sum_k \frac{(2m_kT)^{3/2}}{8\pi^{3/2}}e^{-m_k/T} \equiv |\varepsilon_{vac}| + T^4\chi_1(T). \tag{30}$$

In the deconfined phase one can assume (later confirmed by lattice) (Yu.S. JETP Lett.'92), that

$$D^E(x) = 0 = \sigma_E; \quad D^H(x), D_1^H, D_1^E \neq 0. \tag{31}$$

$$P_2(T) = |\varepsilon_{vac}^{dec}| + T^4(p_{gl} + p_q) \tag{32}$$

Critical line $T_c(\mu)$

$$P_I = |\varepsilon_{vac}| + \chi_1(T) \to \frac{11}{32} G_2$$

$$P_{II} = \frac{11}{32} G_2^{dec} + (p_{gl} + p_q) T^2;$$

$$P_I(T_c) = P_{II}(T_c)$$

$$T_c(\mu) = \left(\frac{\frac{11}{32} \Delta G_2}{p_{gl} + p_q} \right)^{1/4},$$

within 10% $\Delta G_2 \approx \frac{1}{2} G_2$

$$P_{gl}(T_c) = \frac{16}{\pi^2} \sum_{n=1}^{\infty} \frac{1}{n^4} L_{adj}^n \rightarrow \frac{16}{\pi^2} L_{adj}$$

$$p_q(T_c) = \frac{n_f}{\pi^2} \left[\Phi_\nu \left(\frac{\mu - \frac{V_!(T_C)}{2}}{T_c} \right) + \Phi_\nu \left(-\frac{\mu + \frac{V_!(T_C)}{2}}{T_c} \right) \right]$$

$$\Phi_\nu(a) = \int_0^\infty \frac{z^4 dz}{\sqrt{z^2 + \nu^2} \left(e^{\sqrt{z^2+\nu^2} - a} + 1 \right)}$$

$\nu = \frac{m_q}{T}$. Take $m_q = 0$.

Only 2 parameters (input)

ΔG_2 and $V_1(T_c)$.

$$1.\Delta G_2 = G_2(E,H) - G_2(0,H) \approx \frac{1}{2} G_2(E,H)(10\% acc)$$

$$G_2 = \frac{\pi^2}{36}(D^E(0) + D_1^E(0) + D^H(0) + D_1^H(0));$$

$$D_1^E(0) \approx 0.2 D^E(0) \quad (T=0)$$

2. $V_1(T_c) \cong 0.5$ GeV (lattice, analytic) within 10%.

Possible dependence on μ: weak for $\mu \ll$ dilaton mass ≈ 1.5 GeV

lattice data: $V_1 \Rightarrow F^1_{Q\bar{Q}}$

Two limiting cases for $T_c(\mu)$

1). $T_c(\mu \to 0)$: Expanding in $\frac{V_1(T_c)}{8T_c}$

$$T_c = T^{(0)} \left(1 + \frac{V_1(T_c)}{8T_c} + O\left(\frac{V_1(T_c)}{8T_c} \right)^2 \right)$$

with 3% accuracy

$$T_c(0) \approx \frac{1}{2} T^{(0)} \left(1 + \sqrt{1 + \frac{\kappa}{T^{(0)}}} \right), \quad T^{(0)} = \left(\frac{(11 - \frac{2}{3} n_f) \pi^2 \Delta G_2}{384 n_f} \right)^{1/4}. \tag{33}$$

$$\kappa \equiv \frac{1}{2} V_1(\infty, T_c) \cong \frac{1}{2} F^1_{Q\bar{Q}}(\infty, T_c) = 0.25 \;\; GeV.$$

2). End-point: $\mu_c(T \to 0)$

Using asymptotics

$$\Phi_0(a \to \infty) = \frac{a^4}{4} + \frac{\pi^2}{2}a^2 + \frac{7\pi^4}{60} + ...$$

one has

$$\mu_c(T \to 0) = \frac{V_1(T_c)}{2} + (48)^{1/4}T^{(0)}\left(1 - \frac{\pi^2}{2}\frac{T^2}{(\mu_c - \frac{V_1(T_c)}{2})} + \right)$$

For $V_1(T_c) = 0.5$ GeV and $n_f = 2$ one has.

$\frac{\Delta G_2}{0.01\ \mathrm{GeV}^4}$	0.191	0.341	0.57	1
$T_c(\ \mathrm{GeV})\quad n_f = 0$	0.246	0.273	0.298	0.328
$T_c(\ \mathrm{GeV})\quad n_f = 2$	0.168	0.19	0.21	0.236
$T_c(\ \mathrm{GeV})\quad n_f = 3$	0.154	0.172	0.191	0.214
$\mu_c(\ \mathrm{GeV})\quad n_f = 2$	0.576	0.626	0.68	0.742
$\mu_c(\ \mathrm{GeV})\quad n_f = 3$	0.539	0.581	0.629	0.686

Check of predictions vs other data

Possible order parameters are

1.

$$\langle\bar{\psi}\psi\rangle,\ \chi_{chiral} = \frac{\partial^2}{\partial m_q^2}\frac{T}{V}\ln Z \approx \frac{\partial}{\partial m_q}\langle\bar{\psi}\psi\rangle \tag{34}$$

2.

$$\sigma_E(T) \tag{35}$$

3.

$$L_{fund},\quad \chi_L \equiv \langle L_{fund}^2\rangle - \langle L_{fund}\rangle^2$$

$$L_{fund} = \frac{1}{N_c}\langle tr_c P\exp(ig\int_0^{1/T} A_4 dz_4)\rangle \tag{36}$$

Predictions: $\sigma_E(T), \langle\bar{\psi}\psi\rangle$ nonzero for $T < T_c$.

A $V_D(\infty, T) = \infty \rightarrow L_{fund} = 0$ for $T < T_c(n_f = 0)$.

B For $T > T_c$ $\sigma_E(T), \langle\bar{\psi}\psi\rangle$ are zero, L_{fund} nonzero.

C $L_{adj} = (L_{fund})^{9/4}$ since $D^E, P_1^E \sim C_2(adj, fund)$

D First order transition; $T_{deconf} = T_{chiral} = T_c$

comparison to lattice

$n_f = 0$

Kaczmarek et al:calculation of L_{fund}, L_{adj}

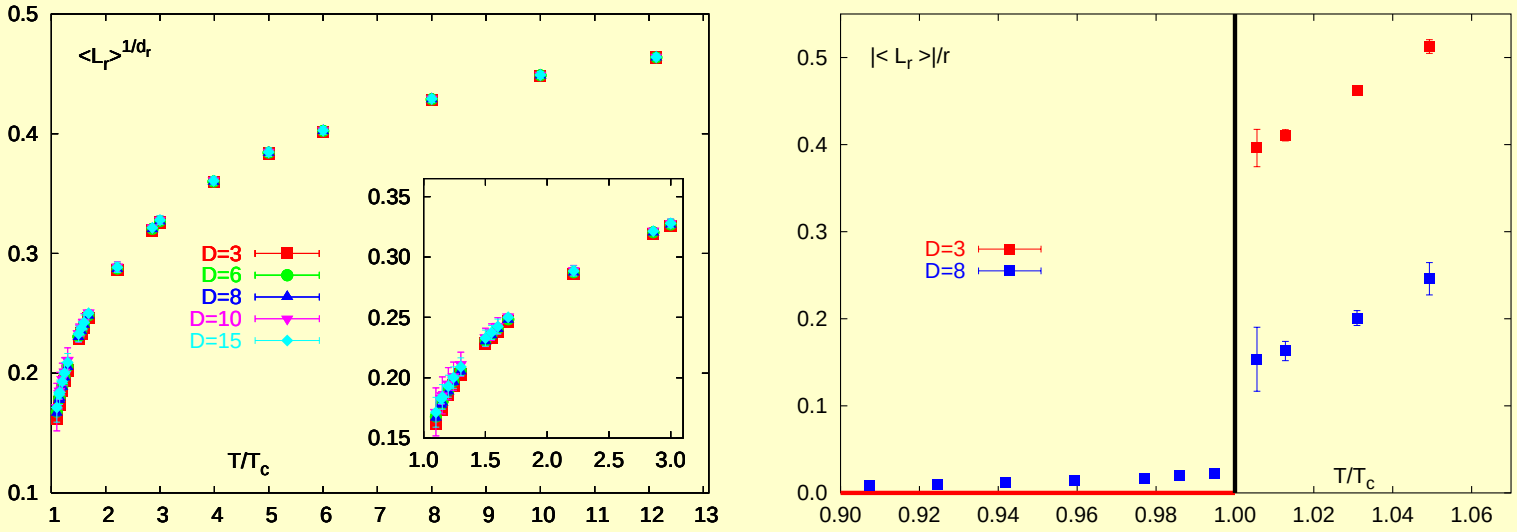

Figure 15: Left: bare Polyakov loops for $r \leq 15$ with cubic spline above T_c. Right: renormalized fundamental and adjoint Polyakov loop for temperatures around T_c.

Agreement: First order transition; Casimir scaling observed

$n_f = 2$ (Di Giacomo et al.)

$$C_V - C_0 = L_s^{\frac{\alpha}{\nu}} \Phi_C(\tau L_s^{\frac{1}{\nu}}, m L_s^{y_h}) \tag{37}$$

and

$$\chi_{\langle\bar{\psi}\psi\rangle} - \chi_0 = L_s^{\frac{\gamma}{\nu}} \Phi_{\langle\bar{\psi}\psi\rangle}(\tau L_s^{\frac{1}{\nu}}, m L_s^{y_h}) \tag{38}$$

	y_h	ν	α	γ	δ
$O(4)$	2.487(3)	0.748(14)	-0.24(6)	1.479(94)	4.852(24)
$O(2)$	2.485(3)	0.668(9)	-0.005(7)	1.317(38)	4.826(12)
MF	$9/4$	$2/3$	0	1	3
$1^{st} Order$	3	$1/3$	1	1	∞

$\tau = 1 - \frac{T}{T_c}, \alpha, \gamma, \nu, y_h$ -crit. indices

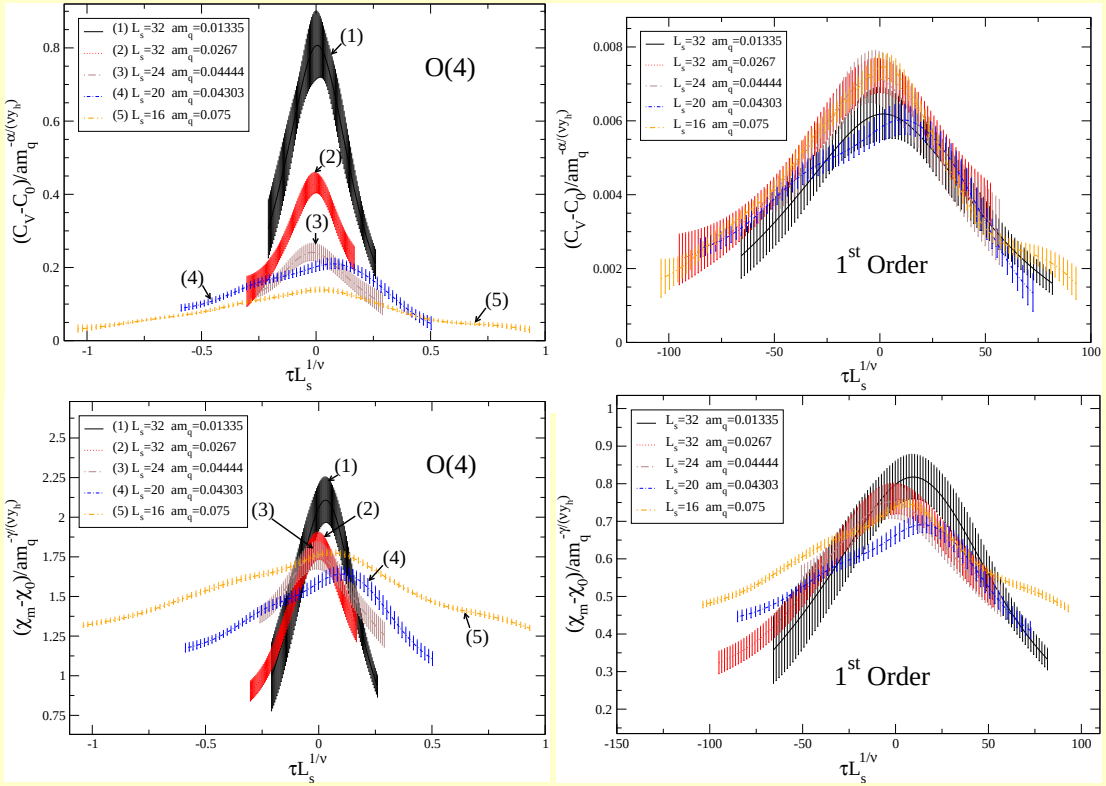

Figure 16: Scaling Eqs. (19),(20) for second order $O(4)$ (left) and first order (right)

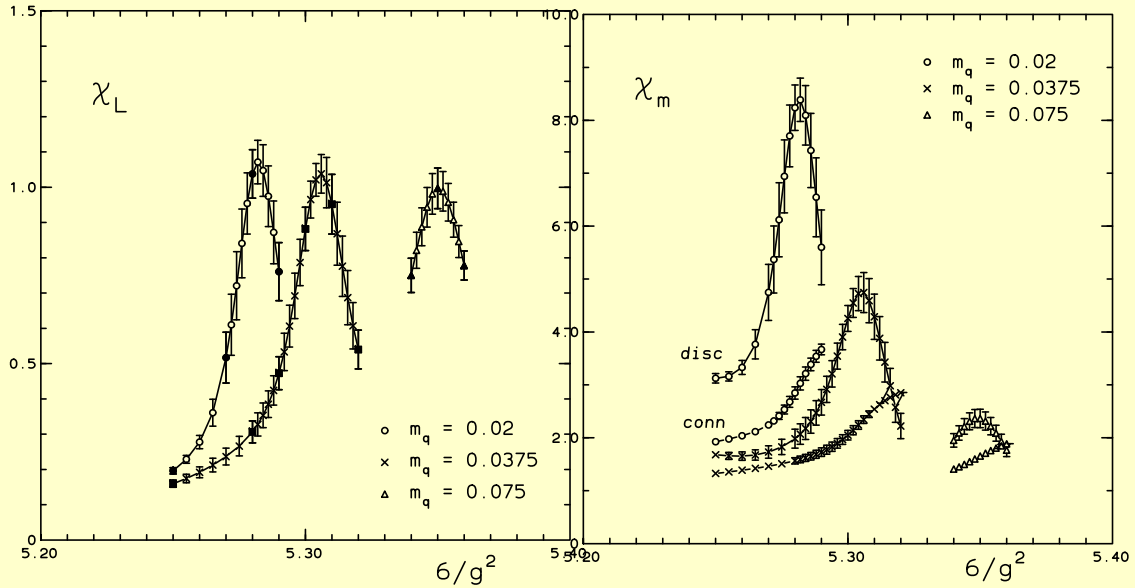

Figure 17: Polyakov loop and chiral susceptibilities versus $\beta = 6/g^2$ in 2-flavour QCD for several values of the quark mass.

One can see coincidence of T_{crit} for each m_q

$n_f = 3$

$m_q = 0$ 1st order

$m_q \neq 0$ crossover (?)

$m_q \to \infty$ 1st order

Conclusions depend on type of quarks used (Wilson, staggered) and discretization.

The slope of $T_c(\mu)$

$$T_c(\mu_B) = T_c(0) - C\frac{\mu_B^2}{T_c^2}, \quad \mu_B = 3\mu_q$$

From general Eq. for $\mu \to 0$

$$p_q(\mu) = \frac{12}{\pi^2} L_{fund} ch \frac{\mu}{T} \cong p_q(0) - (\frac{\mu}{T})^2 \frac{6}{\pi^2} L_{fund}$$

$$T_c(\mu) = \left(\frac{|\Delta\varepsilon_{vac}|}{p_{gl} + p_q(\mu)} \right)^{1/4}$$

One obtains $\kappa \equiv \frac{1}{2} V_1(T_c) \cong 0.25$ GeV

$$C = \frac{1 + \sqrt{1 + \frac{\kappa}{T^{(0)}}}}{144\sqrt{1 + \frac{\kappa}{T^{(0)}}}} = 0.0110(3) \quad \text{for } n_f = 2, 3, 4.$$

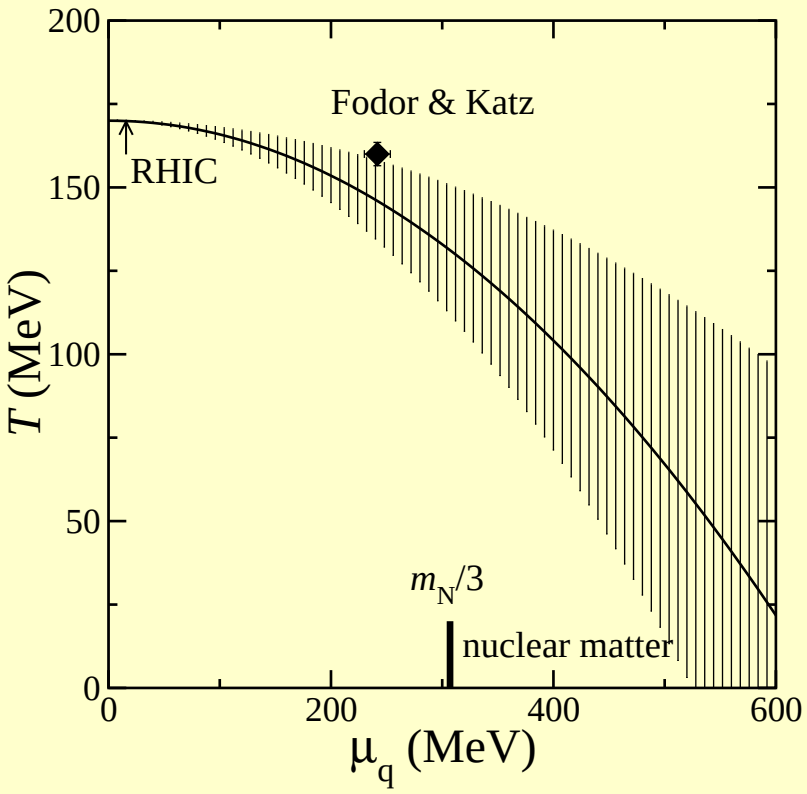

Figure 18: The phase diagram obtained from our reweighting technique. The errors shown are statistical. The diamond is the endpoint of the first order phase transition obtained by Fodor and Katz

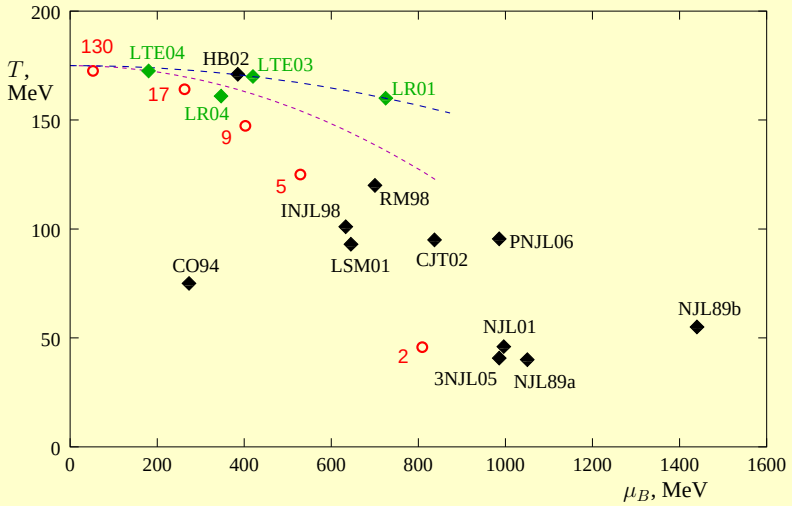

Figure 19: Comparison of predictions for the location of the QCD critical point on the phase diagram. Black points are model predictions: NJLa89, NJLb89, CO94, INJL98, RM98, LSM01, NJL01, HB02, CJT02, 3NJL05, PNJL06. Green points are lattice predictions: LR01, LR04, LTE03, LTE04. The two dashed lines are parabolas with slopes corresponding to lattice predictions of the slope $dT/d\mu_B^2$ of the transition line at $\mu_B = 0$. The red circles are locations of the freezeout points for heavy ion collisions at corresponding center of mass energies per nucleon (indicated by labels in GeV).

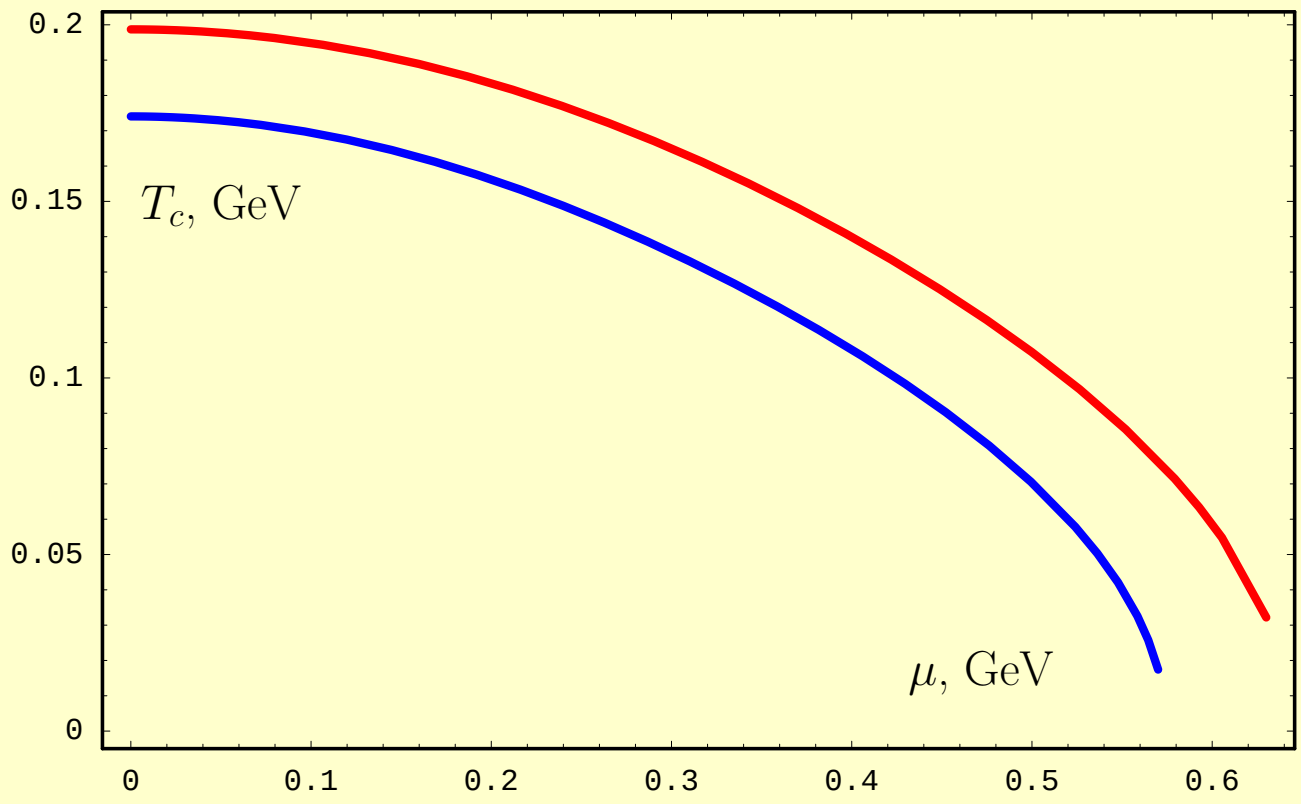

Figure 20:

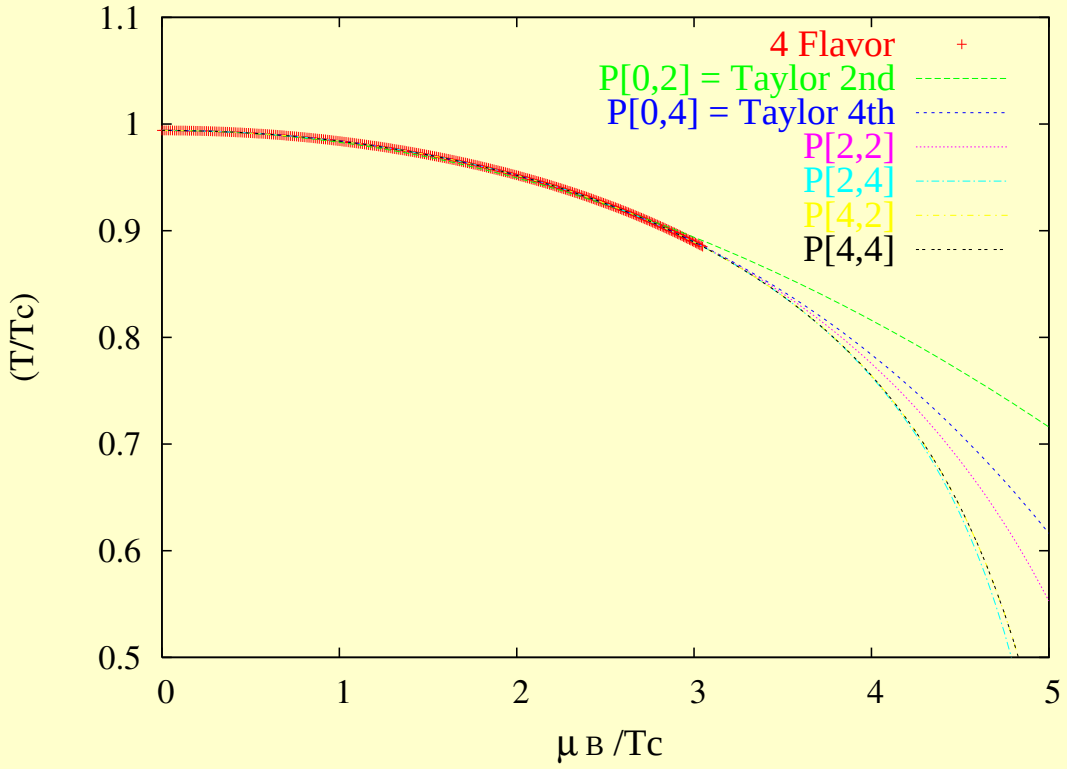
4 Flavor
P[0,2] = Taylor 2nd
P[0,4] = Taylor 4th
P[2,2]
P[2,4]
P[4,2]
P[4,4]
(T/Tc)
μ B /Tc
1.1
1
0.9
0.8
0.7
0.6
0.5
0
1
2
3
4
5

Figure 21:

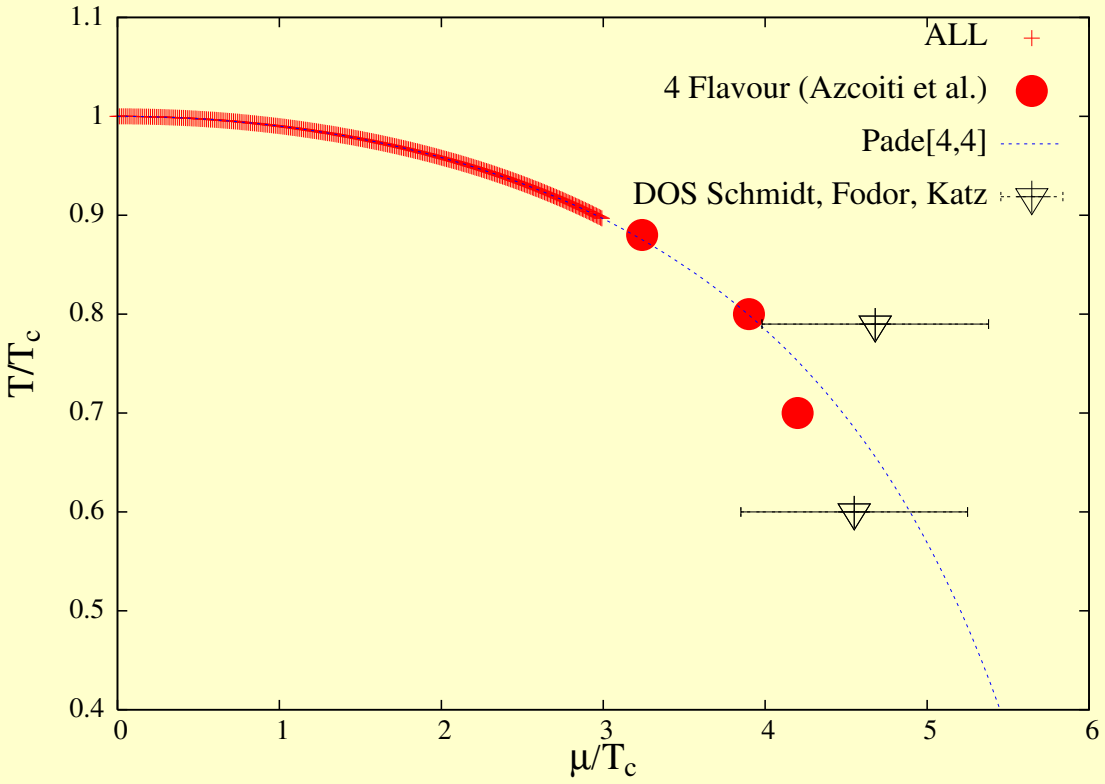
ALL
4 Flavour (Azcoiti et al.)
Pade[4,4]
DOS Schmidt, Fodor, Katz
T/T_c
μ/T_c
1.1
1
0.9
0.8
0.7
0.6
0.5
0.4
0
1
2
3
4
5
6

Figure 22:

$qq, \bar{q}q, gg, 3q$ **interaction at** $T \geq T_c$

Colorelectric binding: D_1^E (Di Giacomo, Meggiolaro, Veselov, Yu.S.)

$$V_1^{(Q\bar{Q})} r, T) = \int_0^{1/T} d\nu (1 - \nu T) \int_0^r \xi d\xi D_1(\sqrt{\xi^2 + \nu^2}) \qquad (39)$$

For any system in repr. D

$$^D V^{(A,B)}(r, T) = \bar{a} V_1^{Q\bar{Q}}(\infty, T) + \bar{b} V_1^{Q\bar{Q}}(r, T)$$

for $(QQ)_3$ $\bar{a} = \bar{b} = \frac{1}{2}$

For $(QQQ)_1$ $V_1^{(QQQ)} = \frac{1}{2} \sum V_1^{(Q\bar{Q})}(\mathbf{r}_i - \mathbf{r}_j, T)$

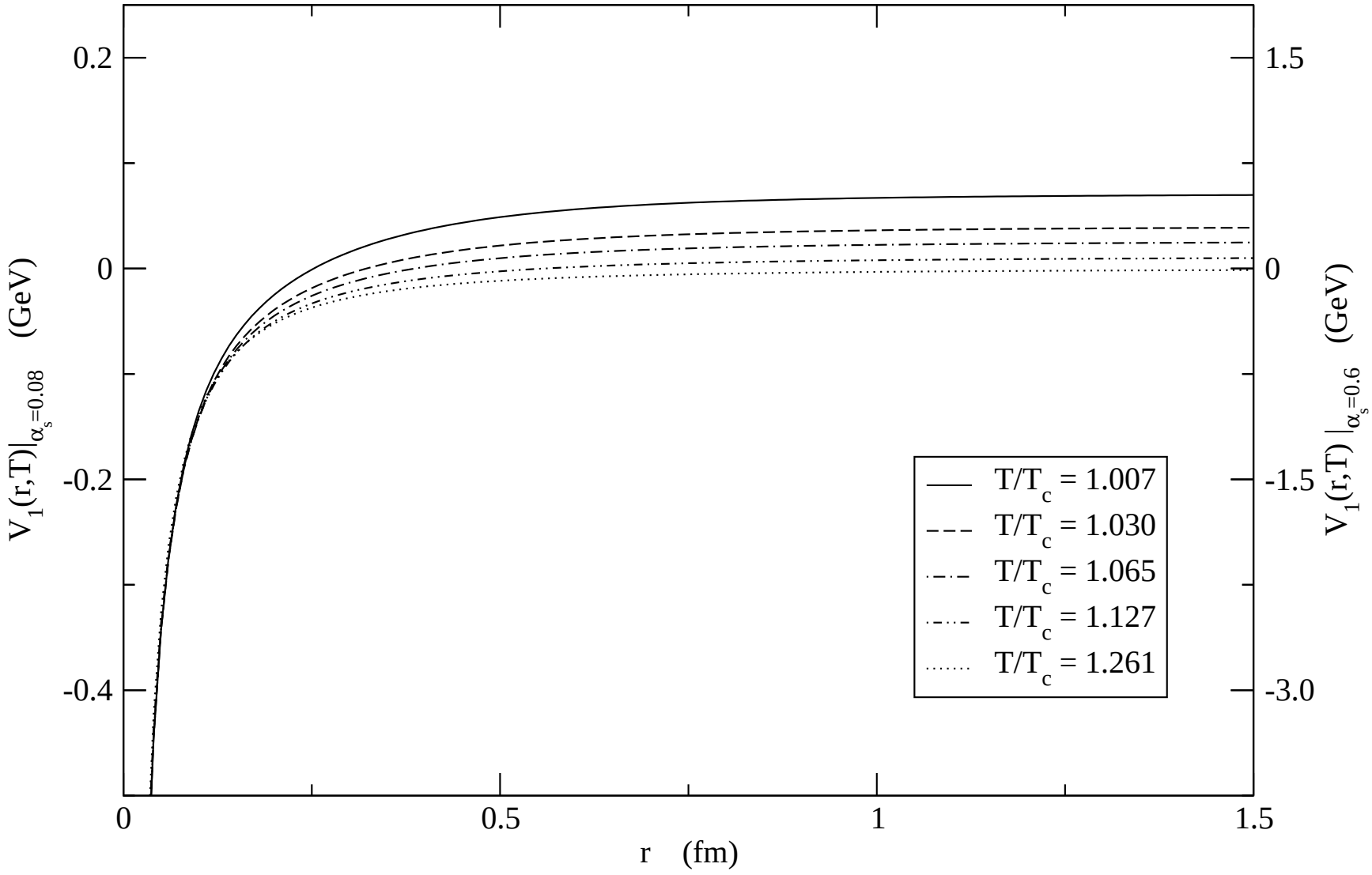
0.2
0
-0.2
-0.4
1.5
0
-1.5
-3.0
0
0.5
1
1.5
r (fm)
$V_1(r,T)|_{\alpha_s=0.08}$ (GeV)
$V_1(r,T)|_{\alpha_s=0.6}$ (GeV)
T/T_c = 1.007
T/T_c = 1.030
T/T_c = 1.065
T/T_c = 1.127
T/T_c = 1.261

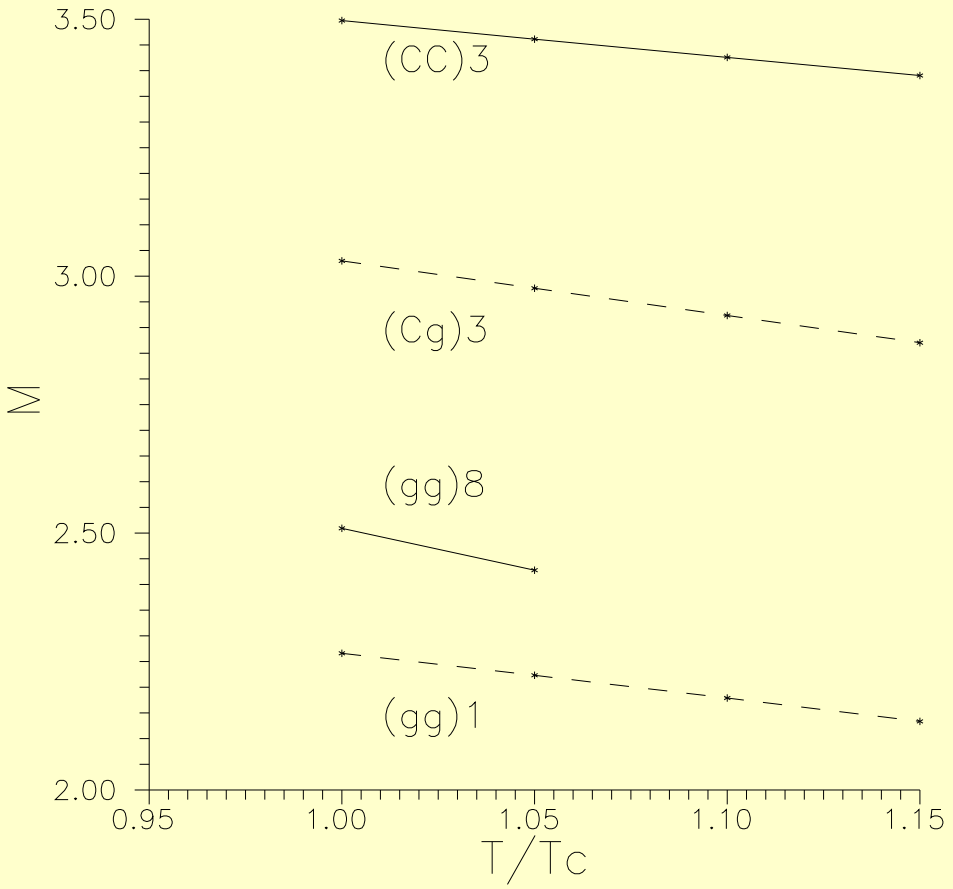

Figure 24:

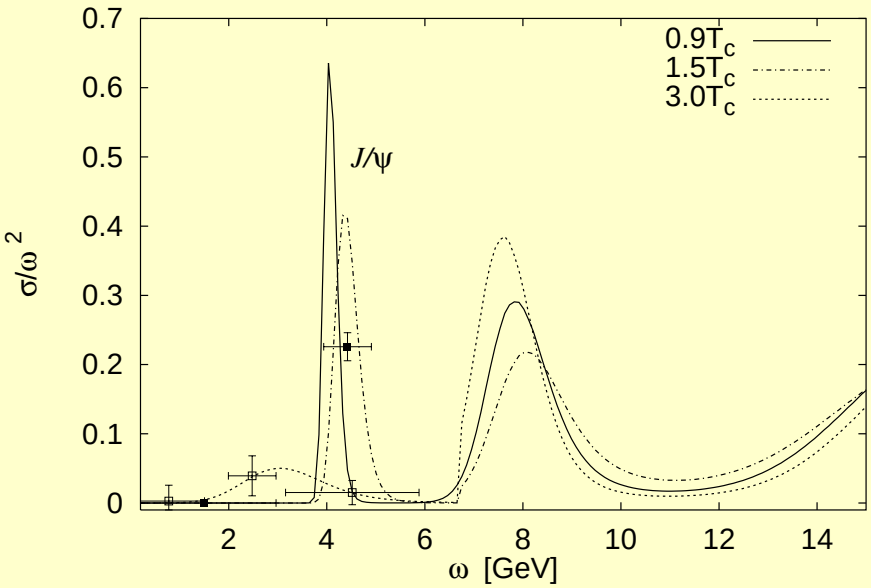
0.7
0.6
0.5
0.4
0.3
0.2
0.1
0
σ/ω 2
0.9Tc
1.5Tc
3.0Tc
J/ψ
2
4
6
8
10
12
14
ω [GeV]

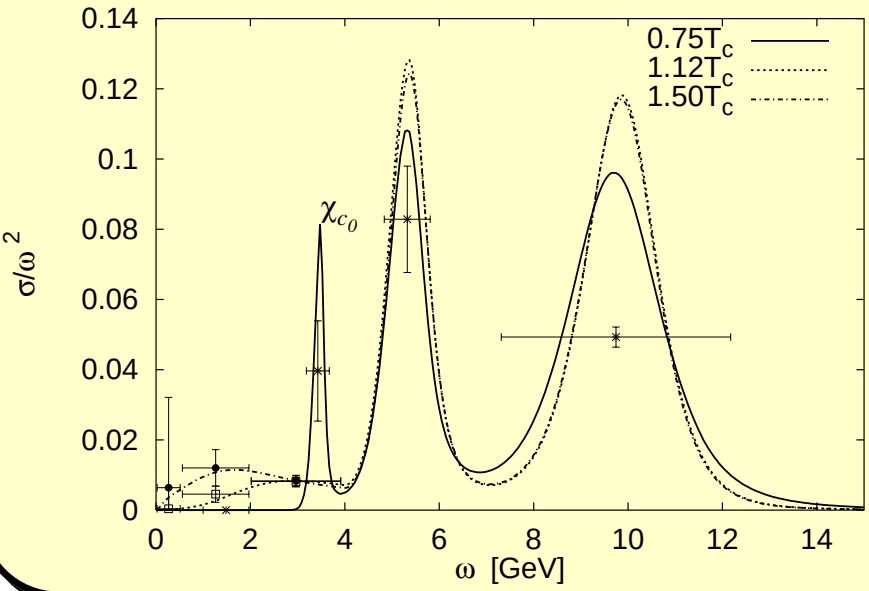
0.14
0.12
0.1
0.08
0.06
0.04
0.02
0
σ/ω 2
0.75Tc
1.12Tc
1.50Tc
χc0
0
2
4
6
8
10
12
14
ω [GeV]

Colormagnetic binding: D^H, D_1^H (Nefediev, Yu.S.)

Hamiltonian of quark–antiquark meson

$$L = -m_1\sqrt{1-\dot{\mathbf{x}}_1^2} - m_2\sqrt{1-\dot{\mathbf{x}}_2^2} - \sigma_E r$$

$$\int_0^1 d\beta \frac{1}{\sqrt{1-[\mathbf{n}\times(\beta\dot{\mathbf{x}}_1+(1-\beta)\dot{\mathbf{x}}_2)]^2}}$$

$$+\sigma_H r \int_0^1 d\beta \frac{[\mathbf{n}\times(\beta\dot{\mathbf{x}}_1+(1-\beta)\dot{\mathbf{x}}_2)]^2}{\sqrt{1-[\mathbf{n}\times(\beta\dot{\mathbf{x}}_1+(1-\beta)\dot{\mathbf{x}}_2)]^2}}$$

$$\underline{m_1 = m_2 = m}$$

$$H_{ll} = \frac{p_r^2 + m^2}{\mu} + \mu + \int_0^1 d\beta \left(\frac{\sigma_1^2 r^2}{2\nu} + \frac{\nu}{2} + \sigma_2 r \right) +$$

$$+ \frac{\mathbf{L}^2}{r^2[\mu + 2\int_0^1 d\beta \nu(\beta - 1/2)^2]}$$

$$\underline{m_1 \to \infty \quad m_2 = m}$$

$$H_{hl} = \frac{p_r^2 + m^2}{2\mu} + \frac{\mu}{2} + \int_0^1 d\beta \left(\frac{\sigma_1^2 r^2}{2\nu} + \frac{\nu}{2} + \sigma_2 r \right) +$$

$$+ \frac{\mathbf{L}^2}{2r^2[\mu + \int_0^1 d\beta \nu \beta^2]}$$

$$\sigma_1(\beta) = \sigma_H + \eta^2(\sigma_H - \sigma_E) \quad \sigma_2(\beta) = 2\eta(\sigma_E - \sigma_H)$$

Spin–orbit interaction above T_c (light–light system)

$$V_{SO}(r) = -\frac{\mathbf{SL}}{\mu r(\mu + 2\langle(\beta - 1/2)^2\rangle)}$$

$$\int_0^\infty d\tau \int_0^r d\lambda D^H(\tau,\lambda)\left(1 - \frac{\lambda}{r}\right)$$

$$\langle(\beta - 1/2)^2\rangle \equiv \int_0^1 d\beta \nu(\beta - 1/2)^2 =$$

$$= \frac{\sigma r}{8y^2}\left(1 + \eta_0^2\right)\left(\frac{1}{\eta_0} - \sqrt{1 - y^2}\right)$$

$$D^H(\tau,\lambda) = \frac{\sigma}{2\pi T_g^2}\exp\left(-\frac{\tau^2 + \lambda^2}{4T_g^2}\right)$$

Effective potentials at $T > T_c$ ($J = l + 1$)

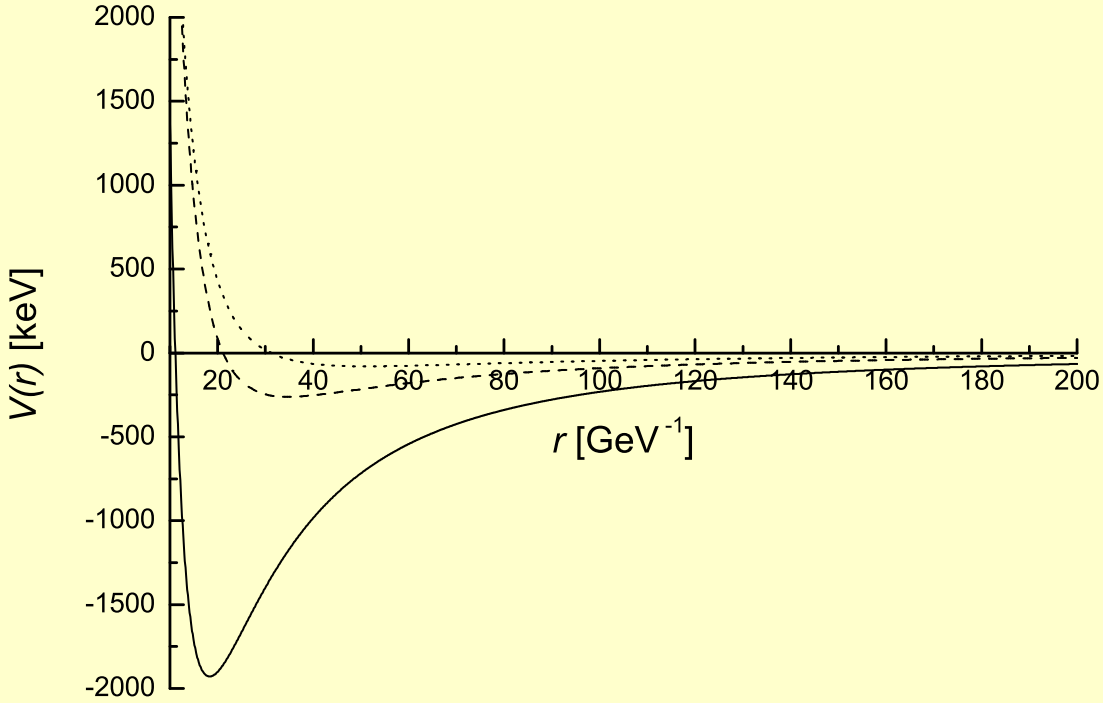

$\mu = 1$GeV (solid) $\mu = 2$GeV (dashed) $\mu = 3$GeV (dotted)

Bound–state problem for light–light system at $T > T_c$

$$M_{n_r l}(\mu) = \frac{m^2}{\mu} + \mu + \varepsilon_{n_r l}(\mu)$$

$$\left.\frac{\partial M_{n_r l}(\mu)}{\partial \mu}\right|_{\mu=\mu_0} = 0 \qquad M_{n_r l} = M_{n_r l}(\mu_0)$$

Investigation of effective potential

$$H_{ll} = \frac{p_r^2 + m^2}{\mu} + \mu + V(r)$$

$$V(r) \simeq \frac{l(l+1)}{(\mu + \sigma r) r^2} - \frac{\sigma l}{2\mu(\mu + \sigma r) r}$$

$$M(m, \mu) = \frac{m^2}{\mu} + \mu + \varepsilon(\mu) \qquad E = M - 2m$$

$$\varepsilon(\mu)[\mathrm{MeV}] \approx -\frac{0.54}{\mu[\mathrm{GeV}]^{2.79}} \Longrightarrow \text{ no extremum at } m \lesssim 0.2\mathrm{GeV}$$

As a result of magnetic confinement at $T > T_c$, one obtains multiple bound states of light quarks with arbitrary large angular momentum and large size with relatively small binding energy – similar to $Z > 137$ electric instability.

Suppression of superconductivity

Diquark nonperturbative interaction

$$V_{QQ}(r) = \frac{1}{2}V_1(\infty, T) + \frac{1}{2}V_1(r, T) = V_1(\infty, T_c) \approx 0.5GeV$$

$$L_q(T) = \exp\left(-\frac{V_1(\infty, T)}{2T}\right)$$

Hence each quark carries Boltzmann factor

$$L_q \approx \exp\left(-\frac{0.25GeV}{T}\right).$$

Dependence on μ is weak-possibly the same factor holds for $\mu \to \mu_{crit}$.

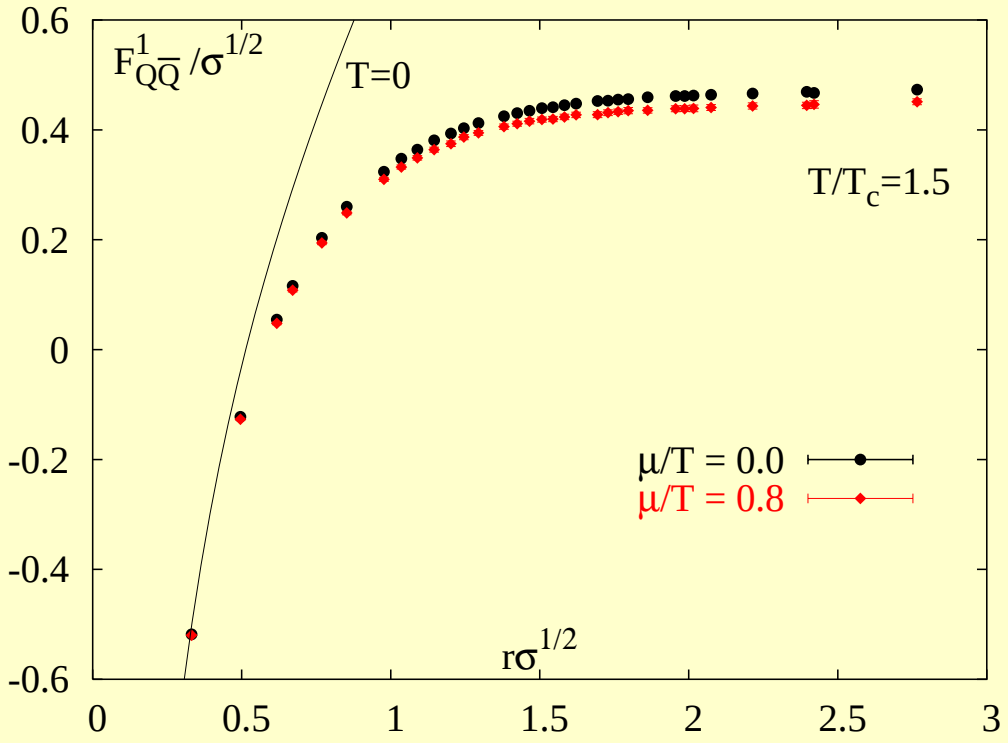

Figure 25:

This fact creates effective mass for quarks $m_{eff} \approx 0.25$ GeV and strongly influences (hinders) diquark condensate formation. In addition strong vacuum colormagnetic field destroys diquark condensate (Agasian, Kerbikov, Shevchenko).

3q at high density

Confining phase at high density

Light q. Linear potential is modified due to $\mu > 0$ at distances $r \leq r_0 \equiv \mu/\sigma$ (Yu.S., '06)

$$\Delta V_{scal} = -\sigma r \theta(r_0 - r),$$
$$\Delta V_{vect} = -2\sigma r \theta(r_0 - r).$$

This leads to baryons of smaller radius and mass, at $\mu \approx 0.4$ GeV, $r_0 \approx 0.3$ fm is the size of nucleon with mass reduced roughly by factor of 2!

EoS and Phase transition strongly changes. It is expected that baryon EoS (Eo as function of density) becomes more stiff.

Conclusions

1. Nonperturbative theory of quark-gluon plasma yields relativistic pictere of dynamics already in the lowest approximation – Vacuum Dominated picture when $q\bar{q}, qqqg, gg$ correlations are neglected. this can be seen in the curves $P(T)$ for $n_f = 0, 2, 3, ...$ and $\mu = 0$.

2. The Vacuum Dominated picture of QCD phase transition gives realistic values for $T_c(\mu)$, which depend only on fundamental parameters– ΔG_2 and $V_1(T_c)$ (expressed via D_1^E or taken from lattice, $V_1(T) \cong F^1_{q\bar{Q}}(\infty, T)$. For $G_2 \sim 0.01$ GeV^4 one has $T_c(0) \sim 0.2$ GeV in good agreement with lattice data.

3. The phase diagram $T_c(\mu)$ obtained in the SLA agrees with majority of lattice data, however behaviour at $\mu \sim \mu_c \sim 0.6$ GeV is not attainable by lattice. Here effects of high baryon density for diquark picture vs $3q, 6q, 9q, ...$ clusters should be elaborated.

Mysteries of deconfinement

1. Why does deconfinement take place at some temperature and density?
2. What is the main dynamical difference between the phases?
3. What are the manifestations of the colour-magnetic confinement?
4. What is the connection between deconfinement and chiral symmetry restoration?
5. What are the values of the QGP transport coefficients (shear and bulk viscosity)?
6. How does the finite density affect the vacuum energy gap?
7. Problem of the phase transition from nuclear matter ro quark matter.
8. Many others....